# Maternal obesity may disrupt offspring metabolism by inducing oocyte genome hyper-methylation via increased DNMTs

Shuo Chao[1#], Jun Lu[1#], Li-Jun Li[1], Hong-Yan Guo[1], Kui-Peng Xu[2], Ning Wang[1], Shu-Xian Zhao[1], Xiao-Wen Jin[1], Shao-Ge Wang[1], Shen Yin[1], Wei Shen[1], Ming-Hui Zhao[1], Gui-An Huang[1], Qing-Yuan Sun[3*], Zhao-Jia Ge[1*]

1. College of Life Sciences, Institute of Reproductive Sciences, Key Laboratory of Animal Reproduction and Germplasm Enhancement in Universities of Shandong, Qingdao Agricultural University, Qingdao 266109, P. R. China;

2. College of Horticulture, Qingdao Agricultural University, Qingdao 266109, P. R. China;

3. Guangzhou Key Laboratory of Metabolic Diseases and Reproductive Health, Guangdong-Hong Kong Metabolism & Reproduction Joint Laboratory, Reproductive Medicine Center, Guangdong Second Provincial General Hospital, Guangzhou 510317, China.

# These authors contributed equally to this work.

* Corresponding author: Zhao-Jia Ge

College of Life Sciences, Qingdao Agricultural University,

Qingdao 266109, P. R. China; +86 15588647272

Email: gejdssd313@163.com; zjge@qau.edu.cn

Qing-Yuan Sun

Reproductive Medicine Center, Guangdong Second Provincial General Hospital, Guangzhou 510317, China. sunqy@gd2h.org.cn.

## Abstract

Maternal obesity has deleterious effects on the process of establishing oocyte DNA methylation; yet the underlying mechanisms remain unclear. In the present study, we found that maternal obesity induced by high-fat diet (HFD) disrupted the genomic methylation of oocytes, and that at least a part of the altered DNA methylation was transmitted to the F2 oocytes and the livers via females. We further examined the metabolome of serum and found that the altered metabolites such as melatonin may play a key role in the disrupted genomic methylation in the oocytes of obese mice. We further found that exogenous melatonin treatment significantly reduced the hyper-methylation of HFD oocytes, and the increased expression of DNMT3a and DNMT1 in HFD oocytes was also decreased. To address how melatonin regulates the expression of DNMTs, the function of melatonin was inhibited or activated upon oocytes. Results revealed that melatonin may regulate the expression of DNMTs via the cAMP/PKA/CREB pathway. These results suggest that maternal obesity induces genomic methylation alterations in oocytes, which can be partly transmitted to F2 in females, and that melatonin is involved in regulating the hyper-methylation of HFD oocytes by increasing the expression of

DNMTs via the cAMP/PKA/CREB pathway.

**Keywords:** Obesity, oocyte, methylation, melatonin, cAMP/PKA/CREB pathway

## Introduction

Obesity has become a global health problem, affecting approximately 13% of the world's adult population, and over 340 million children and adolescents (WHO). This epidemic has profound implications not only for reproductive health but also for the well-being of subsequent generations. Previous studies have demonstrated that maternal obesity reduces the function of the hypothalamic-pituitary-ovarian (HPO) axis (X. Chen, Xiao, Cai, Huang, & Chen, 2022), deteriorates oocyte cytoplasmic quality and nuclear maturation, and disrupts genome methylation (Broughton & Moley, 2017). Reduced expression of *Stella* in oocytes induced by obesity results in global hypo-methylation in zygotes, which has an important contribution to the defective embryo development (Han et al., 2018). Furthermore, progeny of obese females have a higher risk of non-communicable diseases, such as obesity, diabetes, and cardiovascular diseases (Godfrey et al., 2017). Our previous study indicated that obesity altered the methylation status of *Leptin*, which might play a role in the metabolic disorders of female offspring. However, these methylation changes are not detected in the first-generation (F1) oocytes (Ge et al., 2014). The influence of maternal obesity on the genomic methylation of oocytes is still obscure. Thus, more studies

are necessary to explore the role of DNA methylation in mediating the transgenerational transmission of metabolic syndrome induced by female obesity.

Obesity also perturbs glucose and lipid metabolism, which has negative effects on oocyte maturation and embryo development. Elevated levels of circulating free fatty acids in obese females contribute to oocyte lipotoxicity, while concomitantly diminishing mitochondrial function within oocytes (Broughton & Moley, 2017). The decreased melatonin levels are also reported in animals and humans by previous studies (Overberg et al., 2022; Virto et al., 2018). Melatonin has contributions to metabolism and DNA methylation in somatic cells (Davoodvandi, Nikfar, Reiter, & Asemi, 2022). These findings indicate that the disturbed metabolism induced by obesity is closely linked to the compromised oocyte quality and aberrant methylation patterns. This study aims to elucidate the effects of obesity-induced metabolic changes on oocyte genomic methylation and its inhereditary implications in a murine model.

## Results

### Obesity alters the genomic methylation in oocytes

The obese mouse model was induced via a high-fat diet (HFD) (Ge et al., 2014; Han et al., 2018), and mice fed with standard diet were used as a control (CD). The HFD group exhibited a significantly higher average body weight compared to CD group (n>86, Fig. S1A and B). Re-

methylation in oocytes occurs in follicular development and is nearly complete at the germinal vesicle (GV) stage. The 5mC (5-methylcytosine) and 5hmC (5-hydroxymethylcytosine) levels in the GV oocytes of HFD mice were significantly higher than that in the CD group (n>30, Fig. 1A-C). To further explore the effects of maternal obesity on the oocyte methylation, we examined the genomic methylation of metaphase II (MII) oocytes using whole-genome bisulfite sequencing for small samples (WGBS, Novogene, Beijing, China). The information of reads count, mapping rate, conversion rate and sequencing depth was presented in Table S1. We found that global methylation in MII oocytes of HFD group was higher than that in the CD group (Fig. 1D). Methylated cytosine (C) can be classed into three types according to the context in the genome including CG, CHG and CHH (H=A, T or C). The methylated CG have more contributions to regulate gene expression. We found that the CG methylation level in MII oocytes of HFD was significantly higher than that in the CD group (Fig. 1E). Differentially methylated CG distributed across all chromosomes (Fig. S1C). To further analyze the distribution of methylation, each functional region of genes was equally divided into 20 bins, and then the average methylation levels in the functional regions were calculated, respectively. CGIs (CG islands) and CGI shores were predicted using cpgIslandExt and repeat sequences were predicted using RepeatMasker. Results showed that the hyper-methylation was distributed

in the promoter, exon, upstream 2k, and downstream 2k regions (Fig. 1F and Fig. S1D) of genes in HFD oocytes. These findings suggest that maternal obesity results in hyper-genome methylation in oocytes.

**Distribution of differentially methylated regions (DMRs)**

We further analyzed the differentially methylated regions (DMRs) in oocytes, and identified 4340 DMRs between HFD and CD oocytes. These DMRs were defined by the following criteria: the number of CGs $\geq 4$ and the absolute methylation difference $\geq 0.2$. Among these, 2,013 were hyper-DMRs (46.38%), and 2327 were hypo-DMRs (53.62%) (Fig. 1G). These DMRs were distributed across all chromosomes (Fig. 1H). We then annotated DMRs into different genomic regions including promoter, exon, intron, CGI, CGI shore, repeat, TSS (transcription start site), TES (transcription end site), UTR3 (3' end untranslated region), and UTR5 (5' end untranslated region) regions (Fig. S2A), and the average methylation levels of DMRs in these regions were similar between HFD and CD oocytes (Fig. S2B). However, the hypo-DMRs were enriched in the UTR3, repeat, and intron regions compared with hyper-DMRs (Fig. S3).

Methylation level at promoters strongly contributes to the regulation of gene expression. We then analyzed the enrichment of genes with DMRs at promoters in KEGG (Kyoto Encyclopedia of Genes and Genomes) pathways using KOBAS online. Results indicated that the genes with DMRs at promoters were significantly enriched in metabolic pathways

including amino acid metabolism pathways, carbohydrate metabolism pathways, lipid metabolism pathways, and metabolism of cofactors and vitamins pathways (Fig. 1I, Table S2). A total of 35 genes with DMRs at promoters were included in metabolism pathways, and 19 of these genes were with hyper-DMRs and 16 of these genes were with hypo-DMRs (Table S3). These results suggest that the altered methylation in oocytes induced by maternal obesity may play a role in the metabolic disorders in offspring.

**The disturbed methylation may be associated with the transgenerational inheritance of the metabolic disorders through females**

Our recent study demonstrated that disturbed methylation in oocytes caused by uterine undernourishment can be partly transmitted to F2 oocytes via females, which may play a key role in the transgenerational inheritance of metabolic disorders (S. B. Tang et al., 2023). Here, we investigated the inheritance of altered methylation in HFD oocytes. F1 and F2 generations were produced as shown in the schedule in Fig. 1J: HF1 and CF1, female HFD and CD, respectively, were mated with control males; HF2 and CF2, female HF1 and CF1, respectively, were mated with control males. We examined the glucose and insulin tolerance (GTT and ITT), and found that the GTTs and ITTs of F0, F1, and F2 females were impaired (Fig. 2A-C). The inheritance of disrupted metabolism in females

might be associated with the altered DNA methylation of oocytes. To address this question, we first examined the DNA methylation status of DMRs located at the promoters of *Bhlha15* (also known as *Mist1*, basic helix-loop-helix, a transcription factor), *Mgat1* (mannoside acetylglucosaminyltransferase 1), T*aok3* (serine/threonine-protein kinase 3), *Tkt* (transketolase), *Pik3cd* (phosphatidylinositol-4, 5-bisphosphate 3-kinase catalytic subunit delta), and *Pld1* (phospholipase D1) in the HFD and CD oocytes. We found that the methylation levels of hyper-DMRs including *Bhlha15*-DMR, *Mgat1*-DMR, and *Taok3*-DMR in HFD oocytes were significantly higher than in the CD group (Fig. 2D). The methylation level of hypo-DMRs, *Pik3cd-DMR* in HFD oocytes was significantly lower than that in the CD group (Fig. 2D). These results coincide with the genomic sequencing results. Whereas, the methylation level of *Tkt-DMR* (hypo-DMR) in HFD oocytes was higher than that in the CD group, and the methylation level of *Pld1-DMR* (hypo-DMR) was similar between the two groups, which contradicts the genomic sequencing results (Fig. S4A). These findings suggest that some regions are false positives in genomic sequencing. To exclude the effects of somatic cell contamination, we examined the methylation level of paternally imprinted gene *H19,* which was low in both HFD and CD oocytes (Fig. S4B). These findings indicate that the samples are not contaminated by somatic cells.

We then examined the methylation of DMRs in F1 livers using bisulfite

sequencing (BS). Ten livers from five litters were analyzed for each group. Results revealed that the methylation levels of *Bhlha15*-DMR and *Mgat1*-DMR were higher and the methylation level of *Pik3cd*-DMR was lower in HF1 livers than that in CF1 livers (Fig. S5A-C). The methylation level of *Tkt-DMR* in HF1 livers was lower than that in CF1 (Fig. S5D), although it was higher in HFD oocytes compared with CD. This contradiction may be associated with the uterine environment of obesity and the reprogramming during early embryo development. We further examined the expression of several genes with DMRs at promoters, including hyper-methylated genes, such as *Bhlha15*, *Mgat1*, *Dgka*, *Pdpk1* and *Taok3*, and hypo-methylated genes, such as *Igf1*, *Map3k8*, *Pld1*, *Tkt*, *Pik3cd* and *Sphk2*. The expression levels of *Bhlha15*, *Mgat1* and *Pdpk1* were significantly lower and the expression levels of *Map3k8*, *Tkt*, *Pik3cd*, and *Sphk2* were significantly higher in HF1 livers compared to that in CF1 (Fig. S5E and F). The expression trends of *Bhlha15*, *Mgat1*, *Tkt*, and *Pik3cd* were consistent with the methylation status at promoters in F1 livers. The expression of *Dgka*, *Taok3*, *Igf1*, and *Pld1* was not affected in F1 livers (Fig. S4E and F). *Mgat1* is associated with lipid metabolism and obesity (Jacobsson et al., 2012; Johansson et al., 2010), *Tkt* regulates glucose metabolism (Bartakova et al., 2016; Kang et al., 2018), and *Pik3cd* is involved in lipid metabolism and diabetes (Hood, Berger, Freedman, & Law, 2019; Wojcik et al., 2014). These results suggest that the altered methylation in HFD oocytes is partly

transmitted to F1 livers via oocytes, and that the abnormal methylation may be a reason for the disturbed metabolism of HF1.

If the altered methylation in HFD oocytes was inherited by HF1 oocytes, it would be transmitted to F2 generation. Therefore, we examined the methylation of DMRs in F1 oocytes, and results revealed that *Bhlha15*-DMR, *Mgat1*-DMR, and *Taok3*-DMR were significantly hyper-methylated in HF1 oocytes compared with CF1 oocytes (Fig. 2E). The methylation level of *Tkt*-DMR was significantly lower (Fig. S6), and the methylation level of *Pik3cd*-DMR was slightly lower in the HF1 oocytes than that in the CF1 oocytes (Fig. 2E). These results indicate that at least a part of the altered methylation in HFD oocytes is transmitted to F1 oocytes via females.

To confirm the transgenerational inheritance of the altered DNA methylation in HFD oocytes, we examined the methylation levels of DMRs in F2 livers. The methylation of *Bhlha15*-DMR and *Mgat1*-DMR was higher and the methylation level of *Pik3cd*-DMR was lower in HF2 livers than that in CF2 livers (Fig. S7A-C). The methylation of *Tkt*-DMR in HF2 livers was similar to that in CF2 group (Fig. S7D). In addition, the expression levels of *Bhlha15*, *Pdpk1*, and *Mgat1* were significantly lower (Fig. S7E), and the expression levels of *Pld1*, *Pik3cd*, and *Sphk2* were significantly higher in HF2 livers than that in CF2 (Fig. S7F). The expression of the other gene were similar in the livers between HF2 and

CF2 (Fig. S7E and F). These results suggest that at least a part of the altered methylation in HF2 livers may be inherited from HFD oocytes, and that this alteration may be associated with the disrupted metabolism in F2 offspring.

We then examined the methylation of DMRs in F2 oocytes using BS, and found that the hyper-methylation of *Bhlha15*-DMR, *Mgat1*-DMR, and *Taok3*-DMR, and the hypo-methylation of *Pik3cd*-DMR and *Tkt*-DMR were maintained in HF2 oocytes (Fig. 2F).

To better understand the inheritance of the altered methylation, we analyzed the methylation level of DMRs among generations compared with that in HFD oocytes (Fig. 2G). For hyper-DMRs, the methylation of *Bhlha15*-DMR was maintained from HFD oocytes to HF2 oocytes. Compared to those in HFD oocytes, the methylation levels of *Mgat1*-DMR and *Taok3*-DMR were partly transmitted to HF2 oocytes. For hypo-DMRs, the methylation levels of *Tkt*-DMR and *Pik3cd*-DMR in HFD oocytes were inherited by HF2 (Fig. 2G). . We did not examine the methylation level of *Pld1*-DMR in F1 and F2 because it was similar in oocytes between CD and HFD (Fig. 2G). These results suggest that only a part of the altered methylation in HFD oocytes can be transmitted to F2 oocytes, and that disrupted methylation may be a reason for the inheritance of the metabolic disorders in F1 and F2.

**Obesity alters the metabolomics of serum**

Obesity alters the metabolism of glucose, fatty acids, and amino acids, which are essential for oogenesis. Thus, we suppose the altered metabolism may play a key role in the disturbed global methylation in HFD oocytes. We examined the metabolomics of serum using non-targeted approaches (BGI, Wuhan, China). We used LC-MS/MS to identify the variation in metabolites, including amino acids, carbohydrates, lipid, and phenols. The principal component analysis (PCA) showed that the PC1 and PC2, respectively, explained 44.6% and 9.96% of the total metabolite variation, respectively (Fig. 3A). The distribution of extracts between groups was distinguishable (Fig. 3A). We identified 538 differential metabolites based on the PLS-DA (robust orthogonal partial least squares-discriminant analysis) and T-test analysis with the following criteria: VIP (variable importance in projection) $\geqslant 1$, fold change $\geqslant 1.2$ or $\leqslant 0.83$, and p-value<0.05, including 288 upregulated and 250 downregulated metabolites (Fig. 3B). The enrichment of differential metabolites was analyzed using KEGG, which revealed that differential metabolites were significantly enriched in tryptophan and vitamin B6 metabolism (Fig. 3C). The top 20 differential metabolites were presented in Fig. 3D. These results suggest that obesity disturbs the metabolomics of serum.

**Melatonin may play a key role in the genomic hyper-methylation of HFD oocytes**

To investigate the associations between the metabolites and methylation in

oocytes, we identified several differential metabolites in HFD mice, including pyridoxine (vitamin B6), L-methionine, melatonin, and L-tyrosine, which may be associated with the hyper-methylation of oocytes. The concentration of pyridoxine (vitamin B6), L-methionine, and L-tyrosine was significantly increased in HFD serum compared with CD group (Fig. 3D-G). In the methionine cycle, methionine adenosyltransferase catalyzes methionine and ATP into S-adenosyl methionine (SAM) (Shou, Pan, & Chin, 1969) which acts as a universal methyl donor (Lyon, Strippoli, Fang, & Cimmino, 2020). DNA methyltransferases (DNMTs) transfer the methyl group to cytosine and convert SAM to S-adenosyl homocysteine (SAH) which is further degraded to homocysteine (HCY) by SAH hydrolase (D. H. Chen, Wu, Hung, Hsieh, & Li, 2004). During these processes, vitamin B6 serves as a co-factor (Vaccaro & Naser, 2021). Excessive methionine and vitamin B6 intake has been reported to induce hyper-methylation (R. A. Waterland, 2006). These findings indicates that the hyper-methylation in HFD oocytes may be associated with the increased concentrations of methionine and pyridoxine. To confirm this hypothesis, we examined the concentrations of SAM, SAH, and HCY in livers and oocytes, which are crucial intermediate metabolites in the methionine cycle. Results showed that the concentrations of SAM, SAH, and HCY in HFD livers were similar to those in CD livers (Fig. 3H-J), and the concentration of SAM in HFD

oocytes was lower than that in the CD group (Fig. 3K). These results suggest that the higher concentrations of methionine and pyridoxine in the serum of HFD mice may not be the main reason for the genomic hyper-methylation in oocytes.

As presented in Fig. 3D, it is curious that the abundance of genistein, daidzein and dibutylpthalate were also altered in HFD serum compared with those in CD, which might have contributed to the altered DNA methylation in the oocytes. These metabolites might be from the diets or materials used to collect samples. To confirm these results, we examined the concentrations of genistein and dibutylpthalate using ELISA. The results revealed that the concentrations of these metabolites were similar between HFD and CD serum (Fig. S8), which suggest that these metabolites may have no effect on the altered methylation in oocytes.

As presented in Fig. 3D and L, the concentration of melatonin in the HFD serum was significantly lower than that in the CD group. Low concentration of melatonin has also been reported in obese rats (Virto et al., 2018) and humans (Overberg et al., 2022). Exogenous melatonin supplementation reduces body weight and improves lipid and glucose metabolism in both animals and humans (Guan, Wang, Cao, Dong, & Chen, 2021). Melatonin can also inhibit cancer by regulating DNA methylation status (Davoodvandi et al., 2022), improve DNA methylation reprogramming in the development of porcine cloned embryos (Qu et al.,

2020), and affect DNA re-methylation in oocytes (Lan et al., 2018; Saeedabadi, Abazari-Kia, Rajabi, Parivar, & Salehi, 2018; Xiao et al., 2019). This indicates that the reduced melatonin may contribute to the hyper-methylation of HFD oocytes. Here, we found that if HFD mice were treated with exogenous melatonin for 14 days, the genomic hyper-methylation in HFD oocytes was significantly reduced (n≥96 Fig. 3M and N). These results suggest that the reduced melatonin concentration may be involved in regulating the hyper-methylation of HFD oocytes.

**Melatonin regulates genomic methylation of oocytes by increasing the expression of DNMTs via the cAMP/PKA/CREB pathway**

Melatonin receptors (MT1 and 2), which are coupled with inhibitor G-protein (Gi), have been identified in oocytes and granulosa cells (Jin et al., 2022; Wang et al., 2021). Activated Gi inhibits the activation of adenylyl cyclases (ADCYs), resulting in a decrease of cAMP (cyclic adenosine monophosphate), which regulates the activation of protein kinase A (PKA) and CREB (cAMP response element-binding protein) (Wongprayoon & Govitrapong, 2021). Elevated cAMP level increases the expression of DNMTs resulting in hyper-methylation in HL-1 cardiomyocytes (Fang et al., 2015). Hedrich *et al*. reported that CREMα induced hyper-methylation of CD8 cluster via increasing the expression of DNMT3a (Hedrich et al., 2014). We thus supposed that melatonin may regulate genomic methylation in oocytes via increasing the expression of DNMTs through the

cAMP/PKA/CREB pathway (Fig. 4A). To confirm this hypothesis, female C57BL/6 mice fed with normal diet were treated with luzindole, an inhibitor of melatonin receptor, and the global methylation of 5mC and 5hmC was significantly increased in oocytes (n≥49 Fig. 4B-D). Luzindole did not affect the concentration of melatonin in the serum (Fig. S9A). However, excessive melatonin treatment significantly increased the concentration of melatonin in the serum (Fig. S9A) and decreased the methylation levels of 5mC and 5hmC in oocytes (Fig. 4B-D). These findings indicate that melatonin may regulate the re-methylation process in oocytes.

To confirm whether melatonin regulates methylation in oocytes via the cAMP pathway, we examined the expression of ADCYs in oocytes using RT-PCR, and found that ADCY5, 6, and 9 were expressed in oocytes (Fig. S9B). The melatonin antagonist luzindole significantly increased the expression of ADCY6 and ADCY9 in oocytes, and melatonin reduced the expression of ADCY6 (Fig. 4E). However, the expression of ADCY5 was lower in the luzindole and melatonin groups compared with the control (Fig. 4E). In addition, the melatonin antagonist luzindole increased, while melatonin decreased the concentration of cAMP in oocytes, respectively (Fig. 4F). These results suggest that melatonin may regulate the synthesis of cAMP via ADCY6 in oocytes. To further confirm the role of cAMP in regulating the methylation of oocytes, we treated mice with SQ22536, an

inhibitor of ADCYs, and found that this treatment significantly reduced the global methylation of 5mC and the concentration of cAMP in oocytes (n≥51 Fig. 5A-C). Whereas, the ADCYs activator forskolin significantly increased the cAMP concentration and global methylation of 5mC in oocytes (Fig. 5A-C). 8-Bromo-cAMP, a cAMP analogue, also increased the global methylation in oocytes (n≥41 Fig. 5D, E). cAMP functions by activating the downstream protein PKA. When we treated mice with H89 2HCL, a PKA antagonist, the global methylation of 5mC was significantly reduced in oocytes (n≥24 Fig. 5F, G). These results suggest that melatonin may mediate the methylation of oocytes via the cAMP/PKA pathway.

cAMP activates PKA which further phosphorylates CREB to regulate gene expression. In oocytes, DNA re-methylation is regulated by DNMTs including DNMT3a, DNMT3l, and DNMT1. Therefore, we next investigated whether melatonin regulates DNMTs expression via the cAMP/PKA/CREB pathway in oocytes. We examined the expression of CREB1, CREM (cAMP responsive element modulator), CREB3l2 (cAMP responsive element binding protein 3 like 2), and ATF1 (activating transcription factor 1) in oocytes. Results showed that ADCYs activator forskolin treatment significantly increased the mRNA expression of CREB1 and CREM, and that the expression of CREB3l2 and ATF1 was slightly increased (Fig. 6A). In addition, the ADCYs inhibitor SQ22536 significantly reduced the expression of CREB1 and CREB3l2, although the

373 expression of CREM and ATF1 was slightly decreased in oocytes (Fig. 6A).
374 Furthermore, treatment with the ADCYs inhibitor SQ22536 significantly
375 reduced the concentration of pCREB1, but it was increased by forskolin
376 treatment in oocytes (n≥36 Fig. 6B, C). The pCREB1 level was also
377 increased by 8-Bromo-cAMP and decreased by the PKA antagonist H89
378 2HCL in oocytes (n≥28 Fig. 6D-G). These results suggest that the
379 expression and phosphorylation of CREB1 can be regulated by the
380 cAMP/PKA pathway. Yang *et al.* demonstrated that CREB regulated
381 DNMT3a expression in neurons of the dorsal root ganglion by binding to
382 the promoter region (Yang et al., 2021). In the present study, the binding of
383 pCREB1 with relative regions of DNMTs was examined using CUT & Tag
384 assay. Each sample contained 500 GV oocytes, and two replicates were
385 involved. The sequencing result revealed that five fragments including 10
386 pCREB1 binding motifs (predicted using online tool JASPAR, Table S4)
387 were associated with DNMTs, including 3 fragments at intron 1 and distill
388 intergenic regions of DNMT3a, 1 fragment at the promoter region of
389 DNMT1, and 1 fragment at intron 13 of DNMT3l (Table S5). These results
390 suggest that pCREB1 may have contributions to regulate the expression of
391 DNMTs.
392 Next, we investigated the expression of DNMT1, DNMT3a, and DNMT3l
393 in oocytes. The melatonin inhibitor luzindole (slightly) and the ADCYs
394 activator forskolin (significantly) increased the expression of DNMT1 and

DNMT3a, respectively (Fig. 7A, B). Melatonin and the ADCYs inhibitor SQ22536 significantly and slightly reduced the expression of DNMT1 and DNMT3a in oocytes, respectively (Fig. 7A, B). The protein level of DNMT3a in GV oocytes was also significantly increased by 8-Bromo-cAMP and decreased by the PKA antagonist H 89 2HCL, respectively (n≥48 Fig. 7C-F). Although DNMT1 is well known as a maintenance methyltransferase, it also contributes to *de novo* methylation in oocytes (Li et al., 2018). Therefore, we examined the localization of DNMT1 in oocytes, and found that 8-Bromo-cAMP treatment significantly increased the localization of DNMT1 in the nucleus of oocytes, but it was reduced by the PKA antagonist H89 2HCL (n≥22 Fig. 7G-J). When the activation of DNMTs was inhibited by 5-azacytidine, the methylation level in GV oocytes was significantly decreased (n≥43 Fig. S10). These results suggest that melatonin may influence the genomic methylation of oocytes via regulating the expression of DNMT1 and DNMT3a mediated via the cAMP/PKA/CREB pathway.

**Increased DNMTs mediate hyper-methylation of HFD oocytes via cAMP/PKA/CREB pathway**

To explore how melatonin regulates the hyper-methylation of HFD oocytes, we examined the expression of DNMTs. Results showed that maternal obesity in mice significantly increased the expression of DNMT1, DNMT3a, and DNMT3l in oocytes (Fig. 8A). Thus, we aimed to confirm

417 whether the cAMP/PKA/CREB pathway mediated the increased
418 expression of DNMTs in HFD oocytes. We examined the concentration of
419 cAMP in oocytes, and found that maternal obesity significantly increased
420 the concentration of cAMP in oocytes compared with that in CD group (Fig.
421 8B). The mRNA expression of CREB1, but not CREM, in the HFD oocytes
422 was significantly increased compared with that in CD group (Fig. 8C), and
423 the pCREB1 level in HFD oocytes was also significantly increased (n≥49
424 Fig. 8D, E). However, the increased level of pCREB1 was reduced by
425 exogenous melatonin treatment (Fig. 8D, E). When obese females were
426 treated with the PKA antagonist H89 2HCL, both 5mC and pCREB1 levels
427 were significantly reduced in oocytes (n≥17 Fig. 8F-I). These results
428 suggest that reduced melatonin in obese mice may increase the expression
429 of DNMTs via the cAMP/PKA/CREB pathway.
430 The increased expression of DNMT3a (Fig. 8A) may have contributed to
431 the genomic hyper-methylation of HFD oocytes because the primary
432 function of DNMT3a is *de novo* DNA methylation. The *de novo*
433 methylation function of DNMT1 is usually prevented by *Stella* ( also
434 known as *Dppa3* or *PGC7*) in oocytes (Bostick et al., 2007). Nevertheless,
435 maternal obesity significantly reduces the expression of *Stella* in oocytes
436 (Han et al., 2018), which indicates that DNMT1 may also contribute to the
437 hyper-methylation of the HFD oocytes. We found that the localization of
438 DNMT1 in the nuclei of HFD oocyte was significantly increased, which

439 could be reduced by the PKA antagonist H89 2HCL treatment (n≥24 Fig.
440 8J, K). These results suggest that the decreased melatonin induced by
441 maternal obesity increases the expression of DNMTs via the
442 cAMP/PKA/CREB pathway, which results in the hyper-methylation in
443 HFD oocytes.

444 **Discussion**

445 Maternal obesity has negative effects on oocyte quality and offspring
446 health, but the underlying mechanisms are not well understod. In the
447 present study, we found that maternal obesity induced hyper-methylation
448 in oocytes, and that the abnormal methylation, at least in part, is transmitted
449 to F2 oocytes in females, which may be associated with the occurrence and
450 inheritance of metabolic disorders. Maternal obesity induced metabolic
451 changes in the serum. The decreased melatonin in serum may be involved
452 in regulating the hyper-methylation of HFD oocytes by increasing the
453 expression of DNMTs, which is mediated by the cAMP/PKA/CREB
454 pathway.

455 Transgenerational epigenetic inheritance is common in plants, but related
456 investigations in mammals are hindered by epigenetic reprogramming
457 events during gametogenesis and early embryo development (Schmitz &
458 Ecker, 2012; Xavier, Roman, Aitken, & Nixon, 2019). In mammals,
459 isogenic agouti viable yellow ($A^{vy}$) and axin-fused ($Axin^{Fu}$) mice, whose
460 phenotypes are regulated by the DNA methylation level of IAP (intra-

cisternal A particle long terminal repeat) respectively located at the upstream and in intron 6, are solid evidence confirming the transgenerational inheritance of epigenetic modifications (Morgan, Sutherland, Martin, & Whitelaw, 1999; Rakyan, Blewitt, Druker, Preis, & Whitelaw, 2002). Nevertheless, epigenetic modifications can be affected by environmental factors such as metabolic diseases and diet. The intergenerational inheritance of phenotypes and epigenetic changes induced by maternal environmental factors have been confirmed by previous studies (B. Chen et al., 2022; Ge et al., 2014), but there are still many debates about the transgenerational inheritance of epigenetic changes induced by environment. Rats from stressed mothers are more likely to be stressed, and that can be transmitted across generations, but this transgenerational inheritance is not mediated by gametes (Weaver et al., 2004). Females cannot mediate the transgenerational inheritance of hyper-methylation induced by diet in $A^{vy}$ mice (Robert A. Waterland, Travisano, & Tahiliani, 2007), but another study reported that if the $A^{vy}$ allele is from the father, the hyper-methylation induced by diet during pregnancy can be retained in germ cells (Cropley, Suter, Beckman, & Martin, 2006). Anway *et al.* reported that the abnormal spermatogenesis induced by the exposure of vinclozolin during pregnancy can be transmitted across four generations via sperm (Anway, Cupp, Uzumcu, & Skinner, 2005). We previously reported that maternal obesity disturbed DNA methylation status of

483 imprinted genes in oocytes (Ge et al., 2014), but the transgenerational
484 inheritance was not observed. We also demonstrated that disturbed
485 methylation in oocytes induced by undernourishment in utero could be
486 inherited, at least partly, by F2 oocytes via females (S.-B. Tang et al., 2023).
487 Recently, Takahashi *et al.* edited DNA methylation of promoter-associated
488 CGIs, and found that the edited DNA methylation, associated with
489 disrupted metabolism, was stably inherited by multiple generations
490 (Takahashi et al., 2023). In the present study, we found that maternal
491 obesity induced genomic hyper-methylation in oocytes, and that a part of
492 the abnormal methylation was transmitted to F2 via female gametes.
493 Moreover, the transmission of metabolic disorders has also been observed
494 across two generations. These results suggest that the transgenerational
495 inheritance of abnormal methylation induced by maternal obesity, at least
496 in part, can be mediated by oocytes, which may be a reason for the
497 inheritance of metabolic disorders.
498 During the methylation process, the methyl group is donated by SAM
499 which is generated from homocysteine, 5-methyltetrahydrofolate
500 (5mTHF), and methionine. 5mTHF is an intermediate of one-carbon
501 metabolism (Mentch & Locasale, 2016). One-carbon units such as folate
502 and vitamin B12 are crucial for the establishment of methylation (Mentch
503 & Locasale, 2016). Disturbed glucose and lipid metabolism also has a
504 negative influence on DNA methylation (Keller et al., 2014). These

505 indicate that abnormal metabolism induced by maternal obesity (King,
506 2006) may play a key role in the genomic hyper-methylation in oocytes. In
507 the present study, we found that the metabolomics of serum from HFD
508 mice was distinguishable from that of serum from CD mice. Although the
509 concentrations of vitamin B6 and methionine were higher in HFD serum
510 than that in CD, this may not be an important reason for the genomic hyper-
511 methylation in oocytes because the concentrations of SAM, SAH, and
512 HCY in the livers and oocytes was similar between CD and HFD mice. In
513 humans, obesity reduces the melatonin level in circulation (Overberg et al.,
514 2022; Virto et al., 2018). In the present study, we also found that maternal
515 obesity induced by high-fat diet reduced the concentration of melatonin in
516 the serum. Melatonin not only can decrease body weight, but also regulates
517 DNA methylation of somatic cells and germ cells (Davoodvandi et al.,
518 2022; Lan et al., 2018). Nevertheless, the molecular mechanism by which
519 melatonin regulates DNA methylation in oocytes is still unclear. Melatonin
520 has two receptors, MT1 and MT2, both of which have been identified in
521 oocytes (Wang et al., 2021). Melatonin receptors interact with the inhibitor
522 G-protein and can regulate gene expression via the cAMP/PKA/CREB
523 pathway (Wongprayoon & Govitrapong, 2021). CREM and cAMP mediate
524 DNA methylation in somatic cells by regulating the expression of *DNMT3a*
525 (Fang et al., 2015; Hedrich et al., 2014). In neurons, CREB interacts with
526 the promoter of *DNMT3a* to regulate its expression and DNA methylation

(Yang et al., 2021). In the present study, we found that melatonin, which is mediated by the cAMP/PKA/CREB pathway, regulates methylation in oocytes by increasing the expression of DNMT1 and DNMT3a. Similar results were also observed in HFD oocytes. Hyper-methylation of HFD oocytes can be reduced by exogenous melatonin and PKA inhibitors. These suggest that decreased melatonin levels are involved in regulating the genomic hyper-methylation of HFD oocytes by increasing the expression of DNMTs, which is mediated by the cAMP/PKA/CREB pathway.

During follicular development, re-methylation in oocytes is catalyzed mainly by DNMT3a and DNMT3l (Kibe et al., 2021). DNMT1 is usually responsible for maintaining DNA methylation, but DNMT1 also contributes to CG methylation in oocytes (Shirane et al., 2013). During normal oocyte development, DNMT1 is mainly prevented from the nuclei by *Stella*. When the *Stella* level is knocked out, *Uhrf1* (Ubiquitin-like containing PHD Ring Finger 1) moves to the nucleus from the cytoplasm and recruits DNMT1 to chromatin, resulting in hyper-methylation (Li et al., 2018). Maternal obesity significantly deceases the expression of *Stella* in oocytes (Han et al., 2018). These suggest that maternal obesity may induce hyper-methylation in oocytes. In the present study, we found that maternal obesity increased the genomic DNA methylation of GV and MII oocytes, the expression of DNMT1 and its localization at chromatin in GV oocytes. These suggest that reduced *Stella* in HFD oocytes may recruit more

549 DNMT1 into chromatin resulting in hyper-methylation. Nevertheless, Han
550 LS *et al.* reported that maternal obesity has no significant influence on
551 whole genome methylation of GV oocytes and Hou YJ *et al.* reported that
552 maternal obesity reduces whole genome methylation of NSN (no Hoechst-
553 positive rim surrounding the nucleolus) GV oocytes. This contradiction
554 may be associated with the methods used to examine the methylation level
555 and the sample size.
556 In summary, we found that maternal obesity induced genomic hyper-
557 methylation in oocytes and that at least a part of the altered methylation
558 can be transmitted to F2 oocytes, which may be a reason for the inheritance
559 of metabolic disorders. Furthermore, reduced melatonin in HFD mice was
560 involved in regulating the genomic hyper-methylation of oocytes by
561 increasing the expression of DNMTs, and this process was mediated by the
562 cAMP/PKA/CREB pathway. However, there are some limitations for the
563 present study: there is not enough evidence to confirm the role of altered
564 DNA methylation in metabolic disorders in the offspring of obese mothers
565 The molecular mechanisms by which DNA methylation escapes
566 reprogramming in oogenesis have not been elucidated. There are may be
567 other mechanisms involved in regulating genomic hyper-methylation in
568 HFD oocytes. Therefore, more studies are needed in the short future.

569 **Materials and methods**

570 **Mice**

C57BL/6 mice were purchased from Jinan Pengyue Company (Jinan, China). Mice were housed in the controlled room with 12 h light and 12 h dark cycle, and at 23-25℃. The Animal Ethics Committee of Qingdao Agricultural University supported all procedures (QAU201900326).

For the obesity model, female C57BL/6 mice at the age of 4 weeks were randomly divided into two groups fed with high-fat diet (HFD, Research Diets, D12492, USA) and normal diet (CD) for 12 weeks, respectively. We examined the body weight every week. The formulation of the diets is presented in Table S6.

Offspring were produced according to the schedule in Fig.1J. For F1 offspring, female HFD and CD mice were mated with normal adult male C57BL/6 mice, respectively, and the offspring were marked as HF1 and CF1. To avoid the effects of males on methylation, the same males were used to produce F2: female HF1 and CF1 mating with normal males, marked as HF2 and CF2.

**Immunofluorescence**

Briefly, oocytes were fixed with 4% PFA (paraformaldehyde), permeabilized with 0.5% TritonX-100, and blocked with 1% BSA (bovine serum albumin). After that, the oocytes were incubated with primary antibodies overnight at 4℃. The secondary antibodies were stained for 1 h at room temperature. For 5mC and 5hmC staining, the oocytes were treated with 4 N HCl for 10 min after permeabilization, and then transferred into

100mM Tris-HCl for 10 min. After washed 3 times using PBS/BSA with 0.05% Tween 20, the oocytes were blocked with PBS/BSA for 1 h, and incubated with primary antibodies overnight at 4℃. Secondary antibodies were stained for 1 h at room temperature. Then, oocytes were transferred into DAPI with mounting and sealed. Fluorescence signal was examined using a laser scanning confocal microscope (Leica SP5, Germany). The relative fluorescence intensity was examined using Image J.

**Antibodies**

Primary antibodies used in the present study included anti-5mC antibody (Abcam, ab73938), anti-5hmC antibody (Abcam, ab214728), anti-pCREB antibody (Cell Signaling Technology, 9198S), anti-DNMT3a antibody (Active motif, 61478), and anti-DNMT1 antibody (Active motif, 39204).

**Whole-genome bisulfite sequencing and analysis**

Metaphase II (MII) oocytes were collected from the oviduct. For each sample, 100 oocytes from at least 10 mice were pooled together and transferred to lysis buffer. Genomic DNA was fragmented, and the end was repaired. Then, fragmentations were ligated with adapters. Bisulfite treatment was performed using EZ DNA Methylation-Direct (Zymo Research). Lambda DNA was used as a control. After that, the sequencing library was established and sequenced using Illumina HiSeq/NovaSeq (Novogene, China). The raw data quality was evaluated using FastQC, and low quality data and adapters were trimmed using fastp. Clean data were

615 compared to the reference genome mm10. Methylated C site calling was
616 performed using Bismark. Differentially methylated regions (DMRs) were
617 identified using DSS-single. The enrichment of genes in the KEGG
618 pathway was carried out using the online tool KOBAS.

619 **qPCR**

620 Total RNA was extracted from oocytes or tissues using RNAprep Pure
621 Micro Kit (Tiangen, DP420) or RNA Easy Fast Kit (Tiangen, DP451).
622 cDNA was synthesized using Hifair III 1st Strand cDNA Synthesis Kit
623 (Yeasen, China). cDNA was used as templates to examined the relative
624 expression of genes. Housekeeping genes *Ppia* and *Gapdh* were used as
625 references. Relative expression was calculated as $2^{-\Delta\Delta Ct}$.

626 **Bisulfite sequencing (BS)**

627 Each sample included 5 oocytes and at least 20 samples were used for each
628 DMR. The samples were treated as described in a previous study (Ge et al.,
629 2014). Briefly, samples were treated with lysis buffer and 0.3 M NaOH,
630 respectively. After that, samples were embedded in 2% low melting point
631 agarose (Sigma), which was treated with fresh bisulfite solution (2.5 M
632 sodium metabisulfite, Merck; 125 mM hydroquinone, Sigma; pH 5) for 4
633 h. Treated DNA was used as templates to amplify the target fragment using
634 nest-PCR. PCR products were cloned to T-vector and sequenced.
635 Methylation status was analyzed using BiqAnalyzer, which can remove the

636 low conversion rate (<97%) and possible repeat sequences. At least 10
637 available clones was used for each DMR.

638 **Glucose and insulin tolerance**

639 Glucose and insulin tolerance (GTT and ITT) were examined as previously
640 reported (S. B. Tang et al., 2023). Briefly, mice were treated with glucose
641 at 2 g/kg body weight or insulin (Actrapid®, Novo Nordisk) at 10 IU/kg
642 body weight after 16 h or 4 h fasting, respectively. After that, blood glucose
643 was measured by tail blood at 0, 30, 60, 90, and 120 min, respectively.

644 **ELISA**

645 Concentrations of cAMP, SAM, SAH, and HCY were examined using
646 ELISA kits (Jinma Biotechnology Co. Ltd, Shanghai, China) according to
647 the handbook. A standard curve was produced using four-parameters
648 logistics.

649 **Non-target metabolomics in serum**

650 Metabolites in the serum were examined using LC-MS/MS (BGI, Wuhan,
651 China). Raw date were treated with Compound Discoverer 3.1 (Thermo
652 Fisher Scientific, USA). After that, preprocessing of the exported data was
653 performed using metaX. Metabolites were identified according to the
654 databases of BMDB (BGI), mzCloud and ChemSpider (HMDB, KEGG,
655 LipidMaps). Identified metabolites were annotated according to KEGG
656 and HMDB. Differential metabolites were scanned using PCA and PLS-
657 DA combined with fold changes and Student's t test.

## Chemicals

Inhibitors used in the present study included luzindole (Sigma), SQ22536 (Selleck), forskolin (Selleck), H89 2HCL (Selleck), and azacitidine (Selleck). 8-Bromo-cAMP was purchased from Selleck. Melatonin (Sigma) was injected by tail vein for 14 days. The other chemicals were administrated via intraperitoneal injection for 14 days. The control group was injected with the appropriate solutions.

## CUT & Tag and sequencing

For each sample, 500 oocytes were pooled together for this experiment, and two replicates were performed. Library was established using Hyperactive® Universal CUT&Tag Assay Kit (Vazyme, China) according to the manufacturer's instructions. Briefly, oocytes were washed with washing buffer and transferred into tubes with ConA Beads Pro for 10 min at room temperature. The tubes were placed on a magnetic rack for 2 min, and then discarded the supernatant. After that, 50 μl of precooled antibody buffer and primary antibody were added and incubated overnight at 4 ℃. Then, tubes were put on a magnetic rack for 2 min, discarded supernatant, and added 50 μl Dig-wash buffer with secondary antibody (1:100) into tubes incubated at room temperature for 60 min. Samples were washed three times, and then incubated with pA/G-Tnp pro for 1 h at room temperature. After washing, 50 μl of TTBL was added to the samples and incubated at 37℃ for 1 h. Then, 2 μl 10% SDS and DNA Spike-in were

added to the samples, which were incubated at 55 ℃ for 10 min. Supernatant was transferred into a new tube after being putted on a magnetic rack for 2 min. 25 μl DNA Extract Beads Pro was added into supernatant, incubated 20 min at room temperature, and then washed two times with B&W buffer. After that, the DNA Extract Beads Pro was re-suspended in 15 μl dd$H_2O$, and amplified at 60℃ for 20 cycles. Library quality was examined using Qubit, AATI, and QPCR, and then sequenced using NovaSeq 6000 (Novogene, China). Adaptor and low-quality reads were removed from the raw data, and clean data were used for further analysis. Reads were mapped to the mouse reference genome mm39 using Bowtie2. Peak calling was performed using MACS2 at q-value <0.05. The peak was subsequently annotated into related gene regions.

**Statistical analysis**

Average data are presented as mean ± SE (standard error), and the statistical difference was calculated using two-tail independent-samples t test. Methylation level is presented as a percentage, and the statistical difference was calculated using the chi-square test. If p value < 0.05, the statistical difference was considered to be significant.

**Acknowledgement**

This work was supported by the National Natural Science Foundation of China (31872312), National R&D Program of China (2022YFC2703500), the Breeding Plan of Shandong Provincial Qingchuang Research Team

(Innovation Team of Farm Animal Cloning 012–1622001), and the Doctor Foundation of Qingdao Agricultural University (6631116008).

## Conflicts of interest statement

There are no conflicts of interest to declare.

## Data availability

The raw data of sequencing are submitted to the database BGI Sub with No. CRA011654.

Anway, M. D., Cupp, A. S., Uzumcu, M., & Skinner, M. K. (2005). Epigenetic Transgenerational Actions of Endocrine Disruptors and Male Fertility. *Science, 308*(5727), 1466-1469. doi:10.1126/science.1108190

Bartakova, V., Pleskacova, A., Kuricova, K., Pacal, L., Dvorakova, V., Belobradkova, J., . . . Kankova, K. (2016). Dysfunctional protection against advanced glycation due to thiamine metabolism abnormalities in gestational diabetes. *Glycoconj J, 33*(4), 591-598. Retrieved from https://www.ncbi.nlm.nih.gov/pubmed/27287225. doi:10.1007/s10719-016-9688-9

Bostick, M., Kim, J. K., Esteve, P. O., Clark, A., Pradhan, S., & Jacobsen, S. E. (2007). UHRF1 plays a role in maintaining DNA methylation in mammalian cells. *Science, 317*(5845), 1760-1764. Retrieved from https://www.ncbi.nlm.nih.gov/pubmed/17673620. doi:10.1126/science.1147939

Broughton, D. E., & Moley, K. H. (2017). Obesity and female infertility: potential mediators of obesity's impact. *Fertil Steril, 107*(4), 840-847. Retrieved from https://www.ncbi.nlm.nih.gov/pubmed/28292619. doi:10.1016/j.fertnstert.2017.01.017

Chen, B., Du, Y. R., Zhu, H., Sun, M. L., Wang, C., Cheng, Y., . . . Huang, H. (2022). Maternal inheritance of glucose intolerance via oocyte TET3 insufficiency. *Nature, 605*(7911), 761-766. Retrieved from https://www.ncbi.nlm.nih.gov/pubmed/35585240. doi:10.1038/s41586-022-04756-4

Chen, D. H., Wu, K. T., Hung, C. J., Hsieh, M., & Li, C. (2004). Effects of adenosine dialdehyde treatment on in vitro and in vivo stable protein methylation in HeLa cells. *J Biochem, 136*(3), 371-376. Retrieved from https://www.ncbi.nlm.nih.gov/pubmed/15598895. doi:10.1093/jb/mvh131

Chen, X., Xiao, Z., Cai, Y., Huang, L., & Chen, C. (2022). Hypothalamic mechanisms of obesity-associated disturbance of hypothalamic-pituitary-ovarian axis. *Trends Endocrinol Metab, 33*(3), 206-217. Retrieved from https://www.ncbi.nlm.nih.gov/pubmed/35063326. doi:10.1016/j.tem.2021.12.004

Cropley, J. E., Suter, C. M., Beckman, K. B., & Martin, D. I. K. (2006). Germ-line epigenetic modification of the murine Avy allele by nutritional supplementation. *Proceedings of the National Academy of Sciences, 103*(46), 17308-17312. doi:10.1073/pnas.0607090103

Davoodvandi, A., Nikfar, B., Reiter, R. J., & Asemi, Z. (2022). Melatonin and cancer suppression:

insights into its effects on DNA methylation. *Cell Mol Biol Lett, 27*(1), 73. Retrieved from https://www.ncbi.nlm.nih.gov/pubmed/36064311. doi:10.1186/s11658-022-00375-z

Fang, X., Robinson, J., Wang-Hu, J., Jiang, L., Freeman, D. A., Rivkees, S. A., & Wendler, C. C. (2015). cAMP induces hypertrophy and alters DNA methylation in HL-1 cardiomyocytes. *Am J Physiol Cell Physiol, 309*(6), C425-436. Retrieved from https://www.ncbi.nlm.nih.gov/pubmed/26224577. doi:10.1152/ajpcell.00058.2015

Ge, Z. J., Luo, S. M., Lin, F., Liang, Q. X., Huang, L., Wei, Y. C., . . . Sun, Q. Y. (2014). DNA methylation in oocytes and liver of female mice and their offspring: effects of high-fat-diet-induced obesity. *Environ Health Perspect, 122*(2), 159-164. Retrieved from https://www.ncbi.nlm.nih.gov/pubmed/24316659. doi:10.1289/ehp.1307047

Godfrey, K. M., Reynolds, R. M., Prescott, S. L., Nyirenda, M., Jaddoe, V. W., Eriksson, J. G., & Broekman, B. F. (2017). Influence of maternal obesity on the long-term health of offspring. *Lancet Diabetes Endocrinol, 5*(1), 53-64. Retrieved from https://www.ncbi.nlm.nih.gov/pubmed/27743978. doi:10.1016/S2213-8587(16)30107-3

Guan, Q., Wang, Z., Cao, J., Dong, Y., & Chen, Y. (2021). Mechanisms of Melatonin in Obesity: A Review. *Int J Mol Sci, 23*(1). Retrieved from https://www.ncbi.nlm.nih.gov/pubmed/35008644. doi:10.3390/ijms23010218

Han, L., Ren, C., Li, L., Li, X., Ge, J., Wang, H., . . . Wang, Q. (2018). Embryonic defects induced by maternal obesity in mice derive from Stella insufficiency in oocytes. *Nat Genet, 50*(3), 432-442. Retrieved from https://www.ncbi.nlm.nih.gov/pubmed/29459681. doi:10.1038/s41588-018-0055-6

Hedrich, C. M., Crispin, J. C., Rauen, T., Ioannidis, C., Koga, T., Rodriguez Rodriguez, N., . . . Tsokos, G. C. (2014). cAMP responsive element modulator (CREM) alpha mediates chromatin remodeling of CD8 during the generation of CD3+ CD4- CD8- T cells. *J Biol Chem, 289*(4), 2361-2370. Retrieved from https://www.ncbi.nlm.nih.gov/pubmed/24297179. doi:10.1074/jbc.M113.523605

Hood, V. L., Berger, R., Freedman, R., & Law, A. J. (2019). Transcription of PIK3CD in human brain and schizophrenia: regulation by proinflammatory cytokines. *Hum Mol Genet, 28*(19), 3188-3198. Retrieved from https://www.ncbi.nlm.nih.gov/pubmed/31211828. doi:10.1093/hmg/ddz144

Jacobsson, J. A., Rask-Andersen, M., Riserus, U., Moschonis, G., Koumpitski, A., Chrousos, G. P., . . . Fredriksson, R. (2012). Genetic variants near the MGAT1 gene are associated with body weight, BMI and fatty acid metabolism among adults and children. *Int J Obes (Lond), 36*(1), 119-129. Retrieved from https://www.ncbi.nlm.nih.gov/pubmed/21304485. doi:10.1038/ijo.2011.11

Jin, J. X., Sun, J. T., Jiang, C. Q., Cui, H. D., Bian, Y., Lee, S., . . . Liu, Z. H. (2022). Melatonin Regulates Lipid Metabolism in Porcine Cumulus-Oocyte Complexes via the Melatonin Receptor 2. *Antioxidants (Basel), 11*(4). Retrieved from https://www.ncbi.nlm.nih.gov/pubmed/35453372. doi:10.3390/antiox11040687

Johansson, A., Marroni, F., Hayward, C., Franklin, C. S., Kirichenko, A. V., Jonasson, I., . . . Consortium, E. (2010). Linkage and genome-wide association analysis of obesity-related phenotypes: association of weight with the MGAT1 gene. *Obesity (Silver Spring), 18*(4), 803-808. Retrieved from https://www.ncbi.nlm.nih.gov/pubmed/19851299. doi:10.1038/oby.2009.359

783 Kang, H., Jo, A., Kim, H., Khang, R., Lee, J. Y., Kim, H., . . . Shin, J. H. (2018). PARIS reprograms
784 glucose metabolism by HIF-1alpha induction in dopaminergic neurodegeneration.
785 *Biochem Biophys Res Commun, 495*(4), 2498-2504. Retrieved from
786 https://www.ncbi.nlm.nih.gov/pubmed/29287724. doi:10.1016/j.bbrc.2017.12.147
787 Keller, M., Kralisch, S., Rohde, K., Schleinitz, D., Dietrich, A., Schon, M. R., . . . Bottcher, Y. (2014).
788 Global DNA methylation levels in human adipose tissue are related to fat distribution and
789 glucose homeostasis. *Diabetologia, 57*(11), 2374-2383. Retrieved from
790 https://www.ncbi.nlm.nih.gov/pubmed/25145546. doi:10.1007/s00125-014-3356-z
791 Kibe, K., Shirane, K., Ohishi, H., Uemura, S., Toh, H., & Sasaki, H. (2021). The DNMT3A PWWP
792 domain is essential for the normal DNA methylation landscape in mouse somatic cells and
793 oocytes. *PLoS Genet, 17*(5), e1009570. Retrieved from
794 https://www.ncbi.nlm.nih.gov/pubmed/34048432. doi:10.1371/journal.pgen.1009570
795 King, J. C. (2006). Maternal obesity, metabolism, and pregnancy outcomes. *Annu Rev Nutr, 26*,
796 271-291. Retrieved from https://www.ncbi.nlm.nih.gov/pubmed/16704347.
797 doi:10.1146/annurev.nutr.24.012003.132249
798 Lan, M., Han, J., Pan, M. H., Wan, X., Pan, Z. N., & Sun, S. C. (2018). Melatonin protects against
799 defects induced by deoxynivalenol during mouse oocyte maturation. *J Pineal Res, 65*(1),
800 e12477. Retrieved from https://www.ncbi.nlm.nih.gov/pubmed/29453798.
801 doi:10.1111/jpi.12477
802 Li, Y., Zhang, Z., Chen, J., Liu, W., Lai, W., Liu, B., . . . Zhu, B. (2018). Stella safeguards the oocyte
803 methylome by preventing de novo methylation mediated by DNMT1. *Nature, 564*(7734),
804 136-140. Retrieved from https://www.ncbi.nlm.nih.gov/pubmed/30487604.
805 doi:10.1038/s41586-018-0751-5
806 Lyon, P., Strippoli, V., Fang, B., & Cimmino, L. (2020). B Vitamins and One-Carbon Metabolism:
807 Implications in Human Health and Disease. *Nutrients, 12*(9). Retrieved from
808 https://www.ncbi.nlm.nih.gov/pubmed/32961717. doi:10.3390/nu12092867
809 Mentch, S. J., & Locasale, J. W. (2016). One-carbon metabolism and epigenetics: understanding
810 the specificity. *Ann N Y Acad Sci, 1363*(1), 91-98. Retrieved from
811 https://www.ncbi.nlm.nih.gov/pubmed/26647078. doi:10.1111/nyas.12956
812 Morgan, H. D., Sutherland, H. G., Martin, D. I., & Whitelaw, E. (1999). Epigenetic inheritance at the
813 agouti locus in the mouse. *Nat Genet, 23*(3), 314-318. Retrieved from
814 https://www.ncbi.nlm.nih.gov/pubmed/10545949. doi:10.1038/15490
815 Overberg, J., Kalveram, L., Keller, T., Krude, H., Kuhnen, P., & Wiegand, S. (2022). Interactions
816 between nocturnal melatonin secretion, metabolism, and sleeping behavior in
817 adolescents with obesity. *Int J Obes (Lond), 46*(5), 1051-1058. Retrieved from
818 https://www.ncbi.nlm.nih.gov/pubmed/35140394. doi:10.1038/s41366-022-01077-4
819 Qu, J., Sun, M., Wang, X., Song, X., He, H., & Huan, Y. (2020). Melatonin Enhances the Development
820 of Porcine Cloned Embryos by Improving DNA Methylation Reprogramming. *Cell*
821 *Reprogram, 22*(3), 156-166. Retrieved from
822 https://www.ncbi.nlm.nih.gov/pubmed/32207988. doi:10.1089/cell.2019.0103
823 Rakyan, V. K., Blewitt, M. E., Druker, R., Preis, J. I., & Whitelaw, E. (2002). Metastable epialleles in
824 mammals. *Trends Genet, 18*(7), 348-351. Retrieved from
825 https://www.ncbi.nlm.nih.gov/pubmed/12127774. doi:10.1016/s0168-9525(02)02709-9
826 Saeedabadi, S., Abazari-Kia, A. H., Rajabi, H., Parivar, K., & Salehi, M. (2018). Melatonin Improves

827 The Developmental Competence of Goat Oocytes. *Int J Fertil Steril, 12*(2), 157-163.
828 Retrieved from https://www.ncbi.nlm.nih.gov/pubmed/29707934.
829 doi:10.22074/ijfs.2018.5204
830 Schmitz, R. J., & Ecker, J. R. (2012). Epigenetic and epigenomic variation in Arabidopsis thaliana.
831 *Trends Plant Sci, 17*(3), 149-154. Retrieved from
832 https://www.ncbi.nlm.nih.gov/pubmed/22342533. doi:10.1016/j.tplants.2012.01.001
833 Shirane, K., Toh, H., Kobayashi, H., Miura, F., Chiba, H., Ito, T., . . . Sasaki, H. (2013). Mouse oocyte
834 methylomes at base resolution reveal genome-wide accumulation of non-CpG
835 methylation and role of DNA methyltransferases. *PLoS Genet, 9*(4), e1003439. Retrieved
836 from https://www.ncbi.nlm.nih.gov/pubmed/23637617.
837 doi:10.1371/journal.pgen.1003439
838 Shou, L., Pan, F., & Chin, S. (1969). Pancreatic hormones and hepatic methionine
839 adenosyltransferase in the rat. *Proc Soc Exp Biol Med, 131*(3), 1012-1018. Retrieved from
840 https://www.ncbi.nlm.nih.gov/pubmed/5791769. doi:10.3181/00379727-131-34029
841 Takahashi, Y., Morales Valencia, M., Yu, Y., Ouchi, Y., Takahashi, K., Shokhirev, M. N., . . . Izpisua
842 Belmonte, J. C. (2023). Transgenerational inheritance of acquired epigenetic signatures at
843 CpG islands in mice. *Cell, 186*(4), 715-731 e719. Retrieved from
844 https://www.ncbi.nlm.nih.gov/pubmed/36754048. doi:10.1016/j.cell.2022.12.047
845 Tang, S.-B., Zhang, T.-T., Yin, S., Shen, W., Luo, S.-M., Zhao, Y., . . . Ge, Z.-J. (2023). Inheritance of
846 perturbed methylation and metabolism caused by uterine malnutrition via oocytes. *BMC*
847 *Biology, 21*(1). doi:10.1186/s12915-023-01545-x
848 Tang, S. B., Zhang, T. T., Yin, S., Shen, W., Luo, S. M., Zhao, Y., . . . Ge, Z. J. (2023). Inheritance of
849 perturbed methylation and metabolism caused by uterine malnutrition via oocytes. *BMC*
850 *Biol, 21*(1), 43. Retrieved from https://www.ncbi.nlm.nih.gov/pubmed/36829148.
851 doi:10.1186/s12915-023-01545-x
852 Vaccaro, J. A., & Naser, S. A. (2021). The Role of Methyl Donors of the Methionine Cycle in
853 Gastrointestinal Infection and Inflammation. *Healthcare (Basel), 10*(1). Retrieved from
854 https://www.ncbi.nlm.nih.gov/pubmed/35052225. doi:10.3390/healthcare10010061
855 Virto, L., Haugen, H. J., Fernandez-Mateos, P., Cano, P., Gonzalez, J., Jimenez-Ortega, V., . . . Sanz,
856 M. (2018). Melatonin expression in periodontitis and obesity: An experimental in-vivo
857 investigation. *J Periodontal Res, 53*(5), 825-831. Retrieved from
858 https://www.ncbi.nlm.nih.gov/pubmed/29900537. doi:10.1111/jre.12571
859 Wang, J., Zhuo, Z., Ma, X., Liu, Y., Xu, J., He, C., . . . Liu, G. (2021). Melatonin Alleviates the
860 Suppressive Effect of Hypoxanthine on Oocyte Nuclear Maturation and Restores Meiosis
861 via the Melatonin Receptor 1 (MT1)-Mediated Pathway. *Front Cell Dev Biol, 9*, 648148.
862 Retrieved from https://www.ncbi.nlm.nih.gov/pubmed/33937242.
863 doi:10.3389/fcell.2021.648148
864 Waterland, R. A. (2006). Assessing the effects of high methionine intake on DNA methylation. *J*
865 *Nutr, 136*(6 Suppl), 1706S-1710S. Retrieved from
866 https://www.ncbi.nlm.nih.gov/pubmed/16702343. doi:10.1093/jn/136.6.1706S
867 Waterland, R. A., Travisano, M., & Tahiliani, K. G. (2007). Diet-induced hypermethylation at agouti
868 viable yellow is not inherited transgenerationally through the female. *The FASEB Journal,*
869 *21*(12), 3380-3385. doi:10.1096/fj.07-8229com
870 Weaver, I. C., Cervoni, N., Champagne, F. A., D'Alessio, A. C., Sharma, S., Seckl, J. R., . . . Meaney,

M. J. (2004). Epigenetic programming by maternal behavior. *Nat Neurosci, 7*(8), 847-854. Retrieved from https://www.ncbi.nlm.nih.gov/pubmed/15220929. doi:10.1038/nn1276

Wojcik, M., Mac-Marcjanek, K., Wozniak, L. A., Nadel, I., Lewinski, A., & Cypryk, K. (2014). The association of leukocyte phosphatidylinositol 3-kinase delta overexpression with gestational diabetes mellitus (GDM). *Endokrynol Pol, 65*(1), 17-24. Retrieved from https://www.ncbi.nlm.nih.gov/pubmed/24549598. doi:10.5603/EP.2014.0003

Wongprayoon, P., & Govitrapong, P. (2021). Melatonin Receptor as a Drug Target for Neuroprotection. *Curr Mol Pharmacol, 14*(2), 150-164. Retrieved from https://www.ncbi.nlm.nih.gov/pubmed/32316905. doi:10.2174/1874467213666200421160835

Xavier, M. J., Roman, S. D., Aitken, R. J., & Nixon, B. (2019). Transgenerational inheritance: how impacts to the epigenetic and genetic information of parents affect offspring health. *Hum Reprod Update, 25*(5), 518-540. Retrieved from https://www.ncbi.nlm.nih.gov/pubmed/31374565. doi:10.1093/humupd/dmz017

Xiao, P., Nie, J., Wang, X., Lu, K., Lu, S., & Liang, X. (2019). Melatonin alleviates the deterioration of oocytes from mice subjected to repeated superovulation. *J Cell Physiol, 234*(8), 13413-13422. Retrieved from https://www.ncbi.nlm.nih.gov/pubmed/30609033. doi:10.1002/jcp.28018

Yang, Y., Wen, J., Zheng, B., Wu, S., Mao, Q., Liang, L., . . . Tao, Y. X. (2021). CREB Participates in Paclitaxel-Induced Neuropathic Pain Genesis Through Transcriptional Activation of Dnmt3a in Primary Sensory Neurons. *Neurotherapeutics, 18*(1), 586-600. Retrieved from https://www.ncbi.nlm.nih.gov/pubmed/33051852. doi:10.1007/s13311-020-00931-5

## Figure legends

### Figure1 Maternal obesity alters the DNA methylation of oocytes.

(A) Methylation levels of 5mC and 5hmC in oocytes (n>30). 5mC, 5-methylcytosine; 5hmC, 5-hydroxymethylcytosine; DAPI, chromatin.

(B, C) Relative fluorescence intensity of 5mC and 5hmC in GV oocytes.

(D) Genomic methylation level of MII oocytes examined by single-cell whole genome bisulfite sequencing. The control group (CD) has two replicates, and the obesity group (HFD) has three replicates.

(E) Average genomic CG methylation level in MII oocytes. CD, control group; HFD, obesity group; ** means p value < 0.01.

(F) CG methylation levels at different regions in MII oocytes. CGI, CpG island; utr5, 5' untranslated region; utr3, 3' untranslated region; repeat, repeat sequence.

(G) Total differentially methylated regions (DMRs) in oocytes of control and obesity groups. Hyper-DMRs, hypermethylated DMRs; hypo-DMRs, hypomethylated DMRs.

(H) Distribution of DMRs on chromosomes in MII oocytes. Outside-to-in: chromosomes, hyper-DMRs, TEs (transcription end regions), and gene, hypo-DMRs.

(I) KEGG pathway enrichment of genes with DMRs at the promoter regions, and the top 20 pathways are presented.

(J) Schedule of breeding. Female C57BL/6 mice fed with normal (CD) or high-fat diet (HFD) for 12 weeks were marked as F0. F1 was produced by F0 mated with normal males, respectively, and marked as CF1 and HF1; F2 was produced by female F1 mated with normal males and marked as CF2 and HF2, respectively.

**Figure 2 Transgenerational inheritance of metabolic disorders and altered DNA methylation.**

(A-C) Glucose tolerance (GTT) and insulin tolerance ITT) were tested for female F0, F1, and F2, respectively. * $p<0.05$; ** $p<0.01$.

(D-F) DMR methylation at the promoter regions of *Bhlha15*, *Mgat1*, *Taok3*, *Tkt*, and *Pid3cd* in F0, F1, and F2 oocytes was respectively examined using

bisulfite sequencing. At least 10 available clones from 80-100 oocytes were used to calculate the methylation level. White circle, unmethylated CG; black circle, methylated CG. * $p<0.05$; ** $p<0.01$.

(G) Inheritance of altered methylation in different generations was analyzed. * $p<0.05$; ** $p<0.01$.

**Figure 3 Maternal obesity alters metabolome of serum.**

(A) Principal component analysis in CD and HFD mice.

(B) Differential metabolites in HFD serum compared with those in CD group. Red circles, upregulated metabolites; blue circles, downregulated metabolites.

(C) The enrichment of differential metabolites was analyzed using KEGG, and the top 10 enrichment terms are presented.

(D) Heat map of the top 20 differential metabolites in HFD serum.

(E-G) Comparison of the concentrations of pyridoxine, methionine, and tyrosine among the groups. * $p<0.05$; ** $p<0.01$; *** $p<0.001$.

(H-J) Concentrations of SAM, SAH and HCY in the livers were examined by ELISA. Ns, there was no statistical significance between groups.

(K) The concentration of SAM in oocytes was analyzed using ELISA. ** $p<0.01$.

(L) Relative concentration of melatonin in the serum. *** $p<0.001$.

(M) Genomic DNA methylation in oocytes was examined using immunofluorescence. CD, control group; HFD, obesity group;

HFD+melatonin, obese mice were treated with exogenous melatonin for 14 days.

(N) Relative fluorescence intensity of 5mC was examined using Image J (CD, n=109; HFD, n=104; HFD+melatonin, n=96). * $p<0.05$; *** $p<0.001$.

**Figure 4 Melatonin regulates DNA methylation in oocytes.**

(A) Schedule of the possible pathway by which melatonin regulates DNA methylation in oocytes. According to previous studies, we predicted that melatonin might regulate DNA methylation in oocytes via the cAMP/PKA/CREB pathway .

(B) Effects of melatonin and its inhibitor luzindole on oocyte methylation were examined using immunofluorescence.

(C, D) The relative fluorescence intensities of 5mC and 5hmC were analyzed using Image J (5mC: Control, n=81; Luzindole, n=83; Melatonin, n=86. 5hmC: Control, n=64; Luzindole, n=58; Melatonin, n=49). * $p<0.05$; *** $p<0.001$.

(E) The effects of melatonin and its inhibitor luzindole on the expression of adenylate cyclase (ADCY) in oocytes were examined by qPCR. * $p<0.05$; ** $p<0.01$.

(F) The concentration of cAMP in oocytes was examined by ELISA. * $p<0.05$; ** $p<0.01$.

**Figure 5 Role of cAMP in DNA methylation in oocytes.**

(A) Female mice were respectively treated with the ADCY inhibitor

SQ22536 or activator forskolin. Oocyte methylation was examined using immunofluorescence.

(B) The relative intensity of fluorescence in oocytes was analyzed using Image J (Control, n=107; SQ22536, n=51; Forskolin, n=57). ** $p<0.01$; *** $p<0.001$.

(C) cAMP concentration in oocytes was examined using ELISA. * $p<0.05$; ** $p<0.01$.

(D) Female mice were treated with the cAMP analogue 8-Bromo-cAMP, and oocyte methylation was examined using immunofluorescence. The relative fluorescence intensity of 5mC was analyzed using Image J (E) (Control, n=41; 8-Bromo-cAMP, n=42). ** $p<0.01$.

(F, G) Female mice were treated with the PKA (protein kinase A) antagonist H 89 2HCL, and then oocyte methylation was examined using immunofluorescence. The relative fluorescence intensity of 5mC was analyzed using Image J (G) (Control, n=24; H 89 2HCl, n=25). * $p<0.05$.

**Figure 6 Effects of cAMP on CREB1.**

(A) The mRNA expression of cAMP-response element binding (CREB) proteins in oocytes was examined by qPCR. * $p<0.05$.

(B and C) Phosphorylated CREB1 (pCREB1) in oocytes was examined using immunofluorescence, and the relative fluorescence intensity of pCREB1 was examined by Image J (C) (Control, n=36; SQ22536, n=48; Forskolin, n=41). * $p<0.05$; ** $p<0.01$; *** $p<0.001$.

(D and E) After treatment with the cAMP analogue 8-Bromo-cAMP, pCREB1 in oocytes was examined using immunofluorescence. The relative fluorescence intensity was analyzed using Image J (E) (Control, n=28; 8-Bromo-cAMP, n=28). *** $p<0.001$.

**Figure 7 Role of the melatonin/cAMP/PKA pathway in the expression of DNMTs.**

(A) The expression levels of DNMT1, DNMT3a and DNMT3l in oocytes were examined using qPCR after the treatment with SQ22536 and forskolin. * $p<0.05$.

(B) The relative expressions of DNMT1, DNMT3a and DNMT3l in oocytes were examined using qPCR after the treatment with luzindole and melatonin. * $p<0.05$.

(C) After 8-Bromo-cAMP treatment, the relative expression of DNMT3a in oocytes was examined using immunofluorescence and calculated by Image J (D) (Control, n=54; 8-Bromo-cAMP, n=70). ** $p<0.01$.

(E and F) Treatment with the PKA antagonist H 89 2HCL treatment significantly reduced the level of DNMT3a in oocytes examined using immunofluorescence (Control, n=62; H 89 2HCl, n=48). ** $p<0.01$.

(G and H) DNMT1 localization in the oocyte nucleus was examined using immunofluorescence after 8-Bromo-cAMP treatment (Control, n=30; 8-Bromo-cAMP, n=31). *** $p<0.001$.

(I and J) The localization of DNMT1 in oocyte nucleus was reduced by the

treatment with the PKA antagonist H 89 2HCL (Control, n=22; H 89 2HCl, n=28). ** p<0.01.

**Figure 8 Melatonin regulates DNMTs expression via cAMP/PKA/CREB pathway in HFD oocytes.**

(A) The relative expression of DNMT1, DNMT3a, and DNMT3l in HFD oocytes was examined using qPCR. * p<0.05; ** p<0.01.

(B) The concentration of cAMP in HFD oocytes was examined using ELISA. ** p<0.01.

(C) The relative expressions CREB1 and CREM in HFD oocytes were tested using qPCR. * p<0.05; ** p<0.01.

(D and E) The level of pCREB1 in oocytes was examined using immunofluorescence, and the relative fluorescence intensity was calculated by Image J (E) (CD, n=69; HFD, n=49; HFD+melatonin, n=61). HFD, oocytes from obese mice; CD, oocytes from control mice; HFD + melatonin, oocytes from obese mice treated with exogenous melatonin. * p<0.05; *** p<0.001.

(F and G) Treatment with the PKA antagonist H89 2HCL reduced the methylation level of HFD oocytes (CD, n=48; HFD, n=31; HFD+H 89 2HCl, n=27). ** p<0.01; *** p<0.001.

(H and I) The level of pCREB1 in HFD oocytes was also decreased by the treatment with the PKA antagonist H89 2HCL (CD, n=17; HFD, n=17; HFD+H 89 2HCl, n=22). * p<0.05; ** p<0.01; ns, no statistical

significance between groups.

(J and K) Treatment with the PKA antagonist H89 2HCL reduced the localization of DNMT1 in HFD oocytes (CD, n=24; HFD, n=29; HFD+H 89 2HCl, n=25). ** $p<0.01$; *** $p<0.001$; ns, no statistical significance between groups.

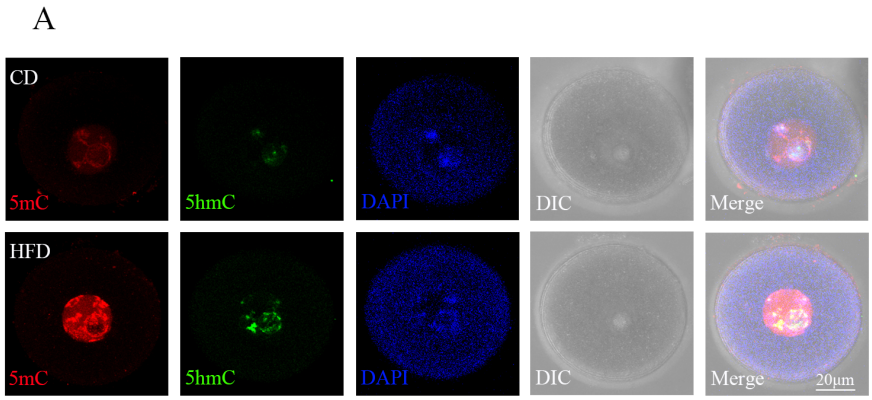
A
CD
5mC
5hmC
DAPI
DIC
Merge
HFD
5mC
5hmC
DAPI
DIC
Merge
20μm

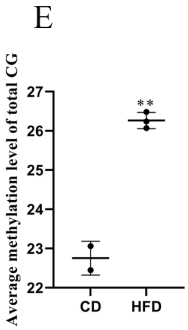
E
Average methylation level of total CG
27
26
25
24
23
22
**
CD
HFD

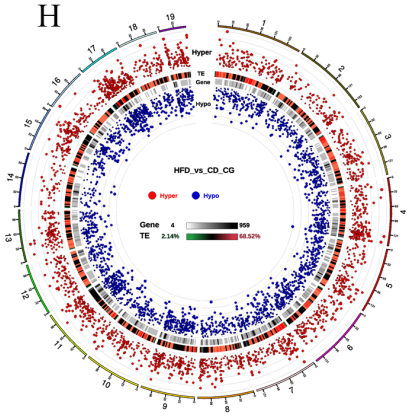
H
Hyper
TE
Gene
Hypo
HFD_vs_CD_CG
Hyper
Hypo
Gene 4 809
TE 2.14% 68.52%

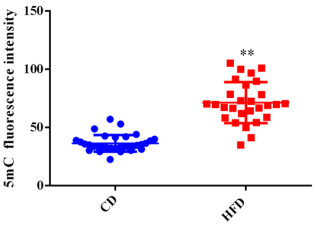
B
5mC fluorescence intensity
150
100
50
0
**
CD
HFD

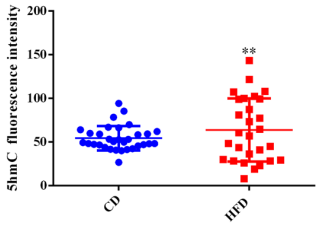
C
5hmC fluorescence intensity
200
150
100
50
0
**
CD
HFD

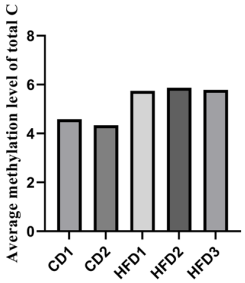
D
Average methylation level of total C
8
6
4
2
0
CD1
CD2
HFD1
HFD2
HFD3

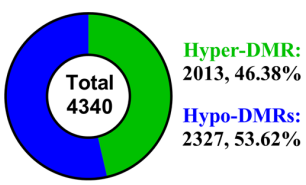
G
Total
4340
Hyper-DMR:
2013, 46.38%
Hypo-DMRs:
2327, 53.62%

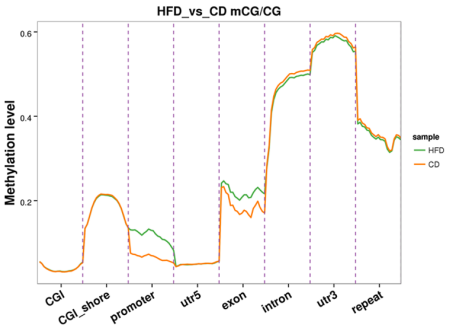
F
HFD_vs_CD mCG/CG
Methylation level
0.6
0.4
0.2
sample
HFD
CD
CGI
CGI_shore
promoter
utr5
exon
intron
utr3
repeat

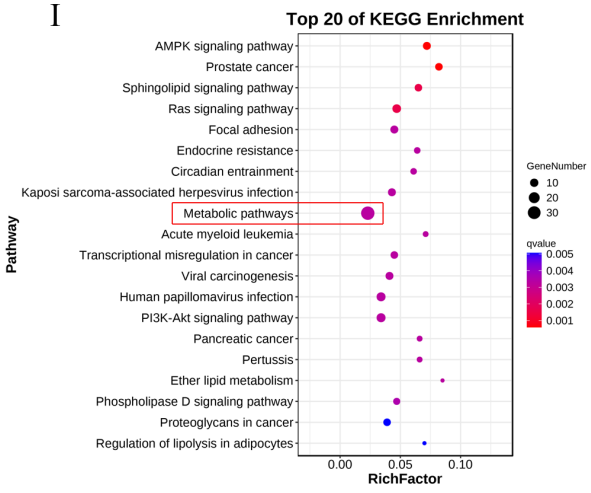
I
Top 20 of KEGG Enrichment
AMPK signaling pathway
Prostate cancer
Sphingolipid signaling pathway
Ras signaling pathway
Focal adhesion
Endocrine resistance
Circadian entrainment
Kaposi sarcoma-associated herpesvirus infection
Metabolic pathways
Acute myeloid leukemia
Transcriptional misregulation in cancer
Viral carcinogenesis
Human papillomavirus infection
PI3K-Akt signaling pathway
Pancreatic cancer
Pertussis
Ether lipid metabolism
Phospholipase D signaling pathway
Proteoglycans in cancer
Regulation of lipolysis in adipocytes
Pathway
0.00
0.05
0.10
RichFactor
GeneNumber
10
20
30
qvalue
0.005
0.004
0.003
0.002
0.001


J
Normal or high-fat diets
4 weeks
12 weeks
12 weeks
CD female
Male
HFD female
F0
F1
CF1 female
HF1 female
F2
CF2 female
HF2 female

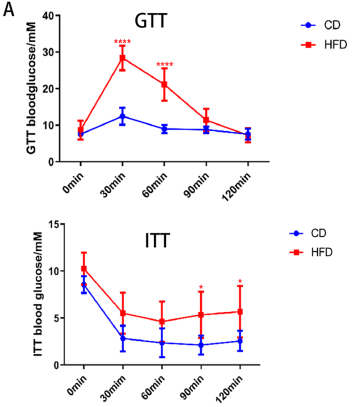


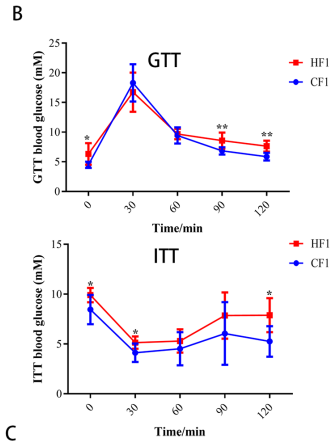


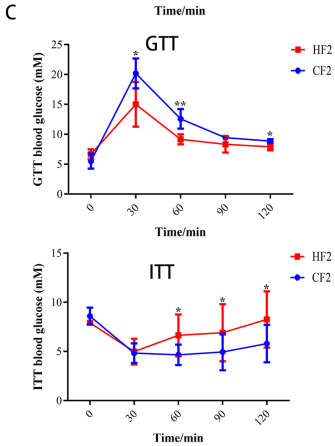


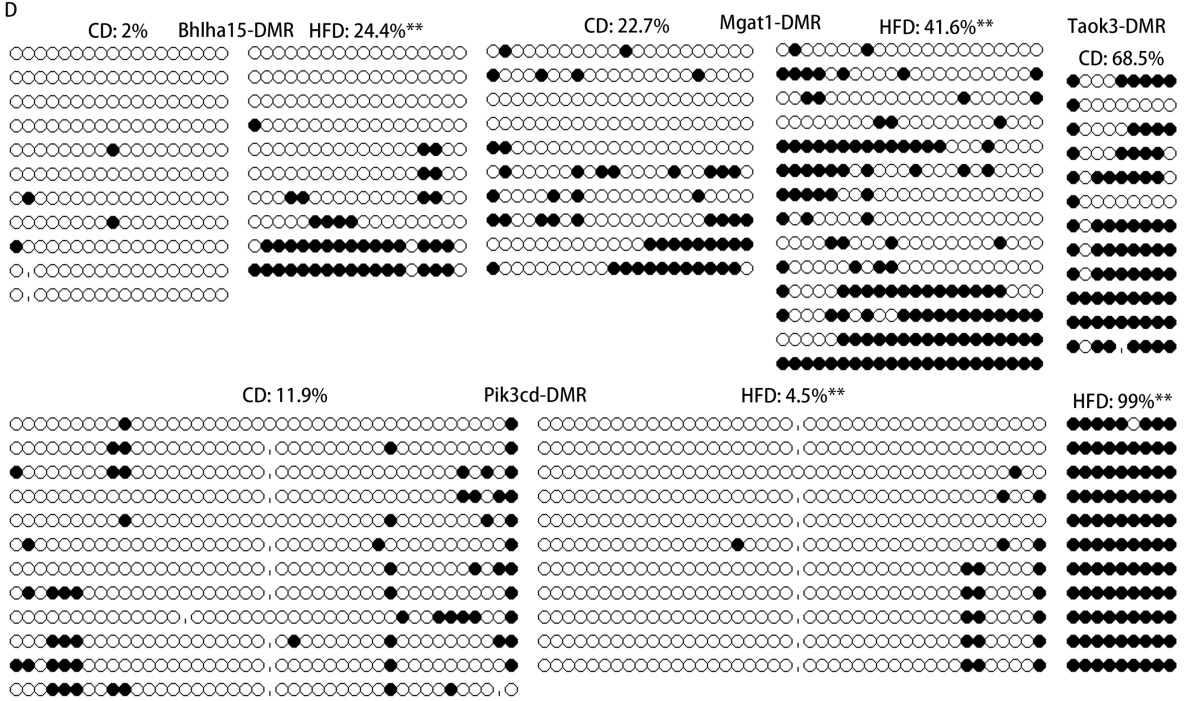


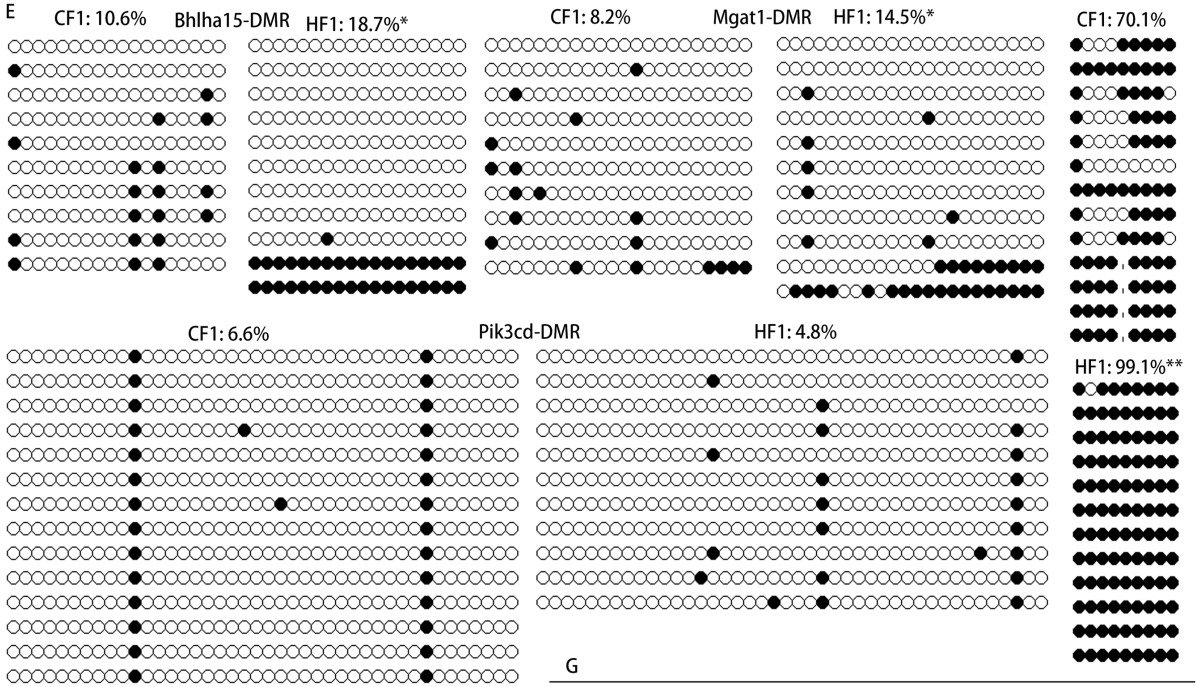


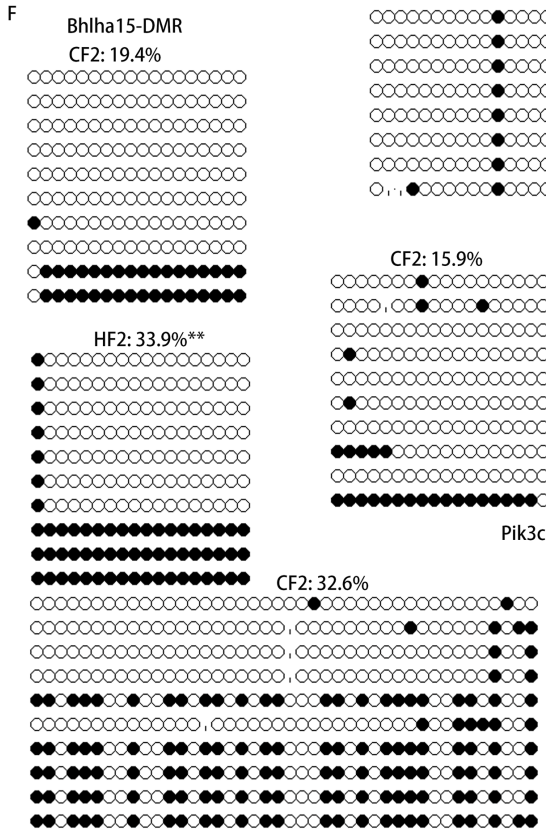


G

| Generation | Tissue | Hyper-DMRs | | | Hypo-DMRs | | |
|---|---|---|---|---|---|---|---|
| | | Bhlha15 | Mgat1 | Taok3 | Tkt | Pik3cd | Pld1 |
| F0 | HFD oocyte | 24.40% | 41.60% | 99% | 7.70% | 4.50% | 98.80% |
| F1 | Liver | 22.20% | 31.4%* | | 0.5%** | 5% | |
| | Oocyte | 18.70% | 14.5%** | 99.10% | 6.40% | 4.80% | |
| F2 | Liver | 21.70% | 26.4%** | | 1.5%** | 3.10% | |
| | Oocyte | 33.90% | 25%** | 84.6%** | 0.5%** | 12.1%** | |

A

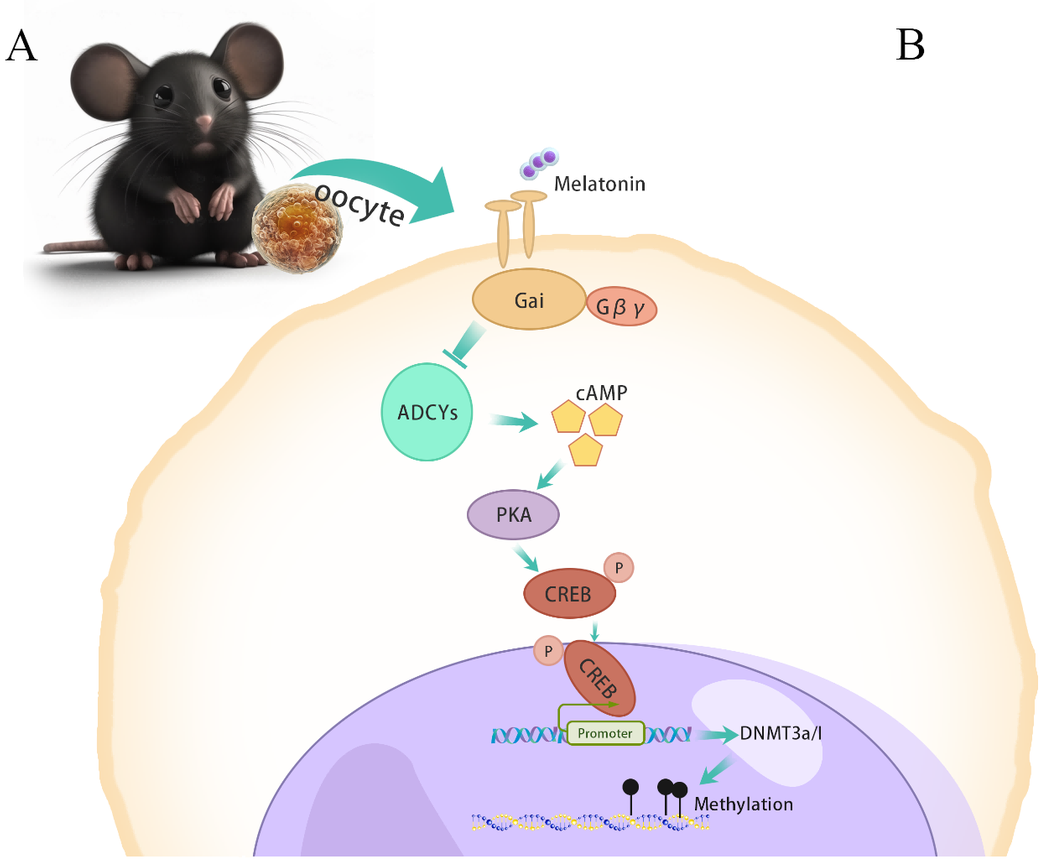
Oocyte
Melatonin
Gai
Gβγ
ADCYs
cAMP
PKA
CREB
P
CREB
P
Promoter
DNMT3a/l
Methylation

B

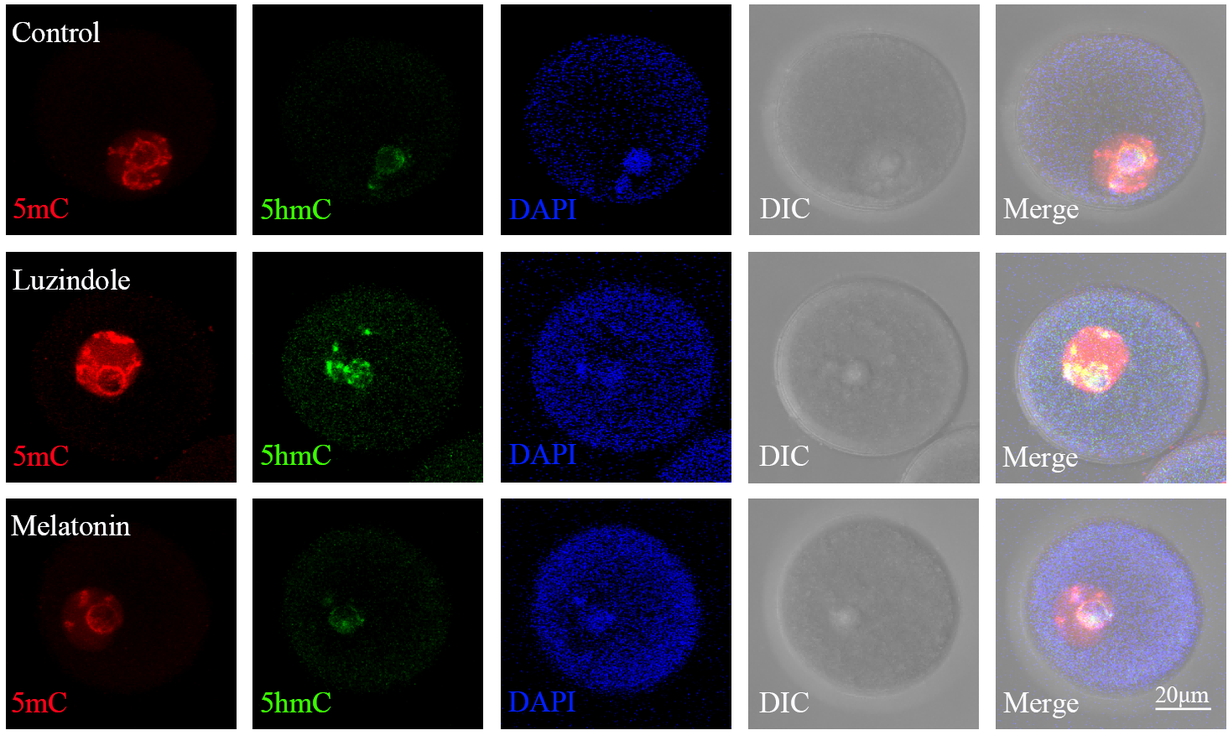
Control
5mC
5hmC
DAPI
DIC
Merge
Luzindole
5mC
5hmC
DAPI
DIC
Merge
Melatonin
5mC
5hmC
DAPI
DIC
Merge
20μm

C

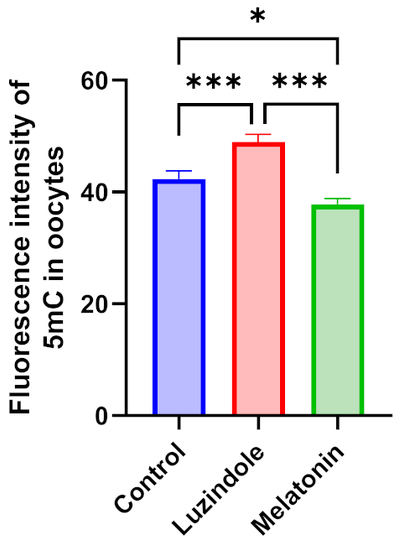
Fluorescence intensity of 5mC in oocytes
60
40
20
0
*
***
***
Control
Luzindole
Melatonin

D

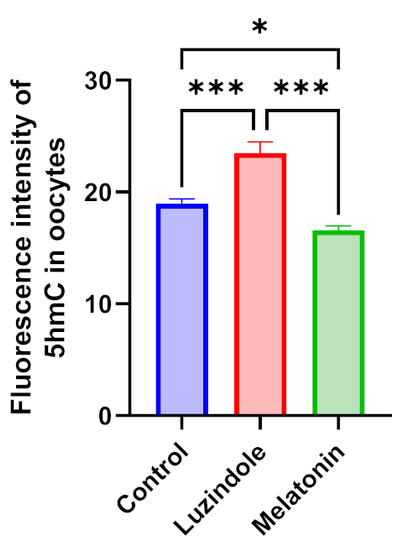
Fluorescence intensity of 5hmC in oocytes
30
20
10
0
*
***
***
Control
Luzindole
Melatonin

E

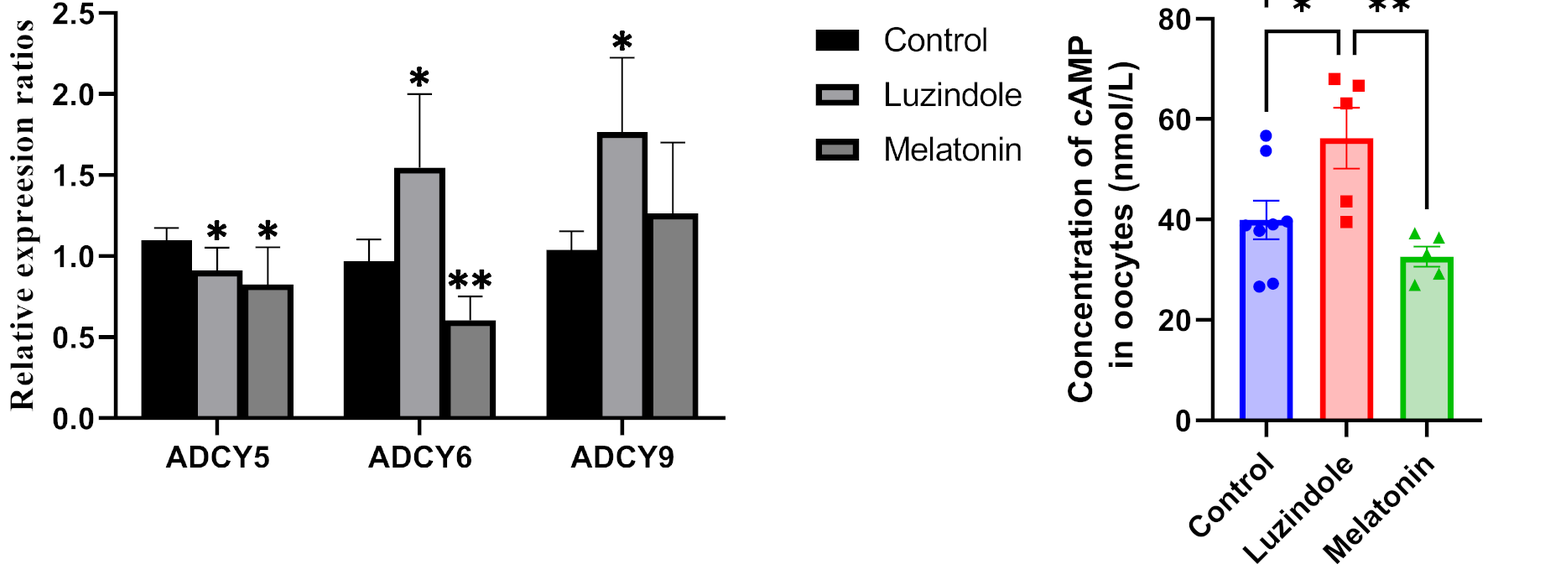
Relative expreesion ratios
2.5
2.0
1.5
1.0
0.5
0.0
*
*
*
**
*
ADCY5
ADCY6
ADCY9
Control
Luzindole
Melatonin

F


ns
*
**
Concentration of cAMP in oocytes (nmol/L)
80
60
40
20
0
Control
Luzindole
Melatonin

A

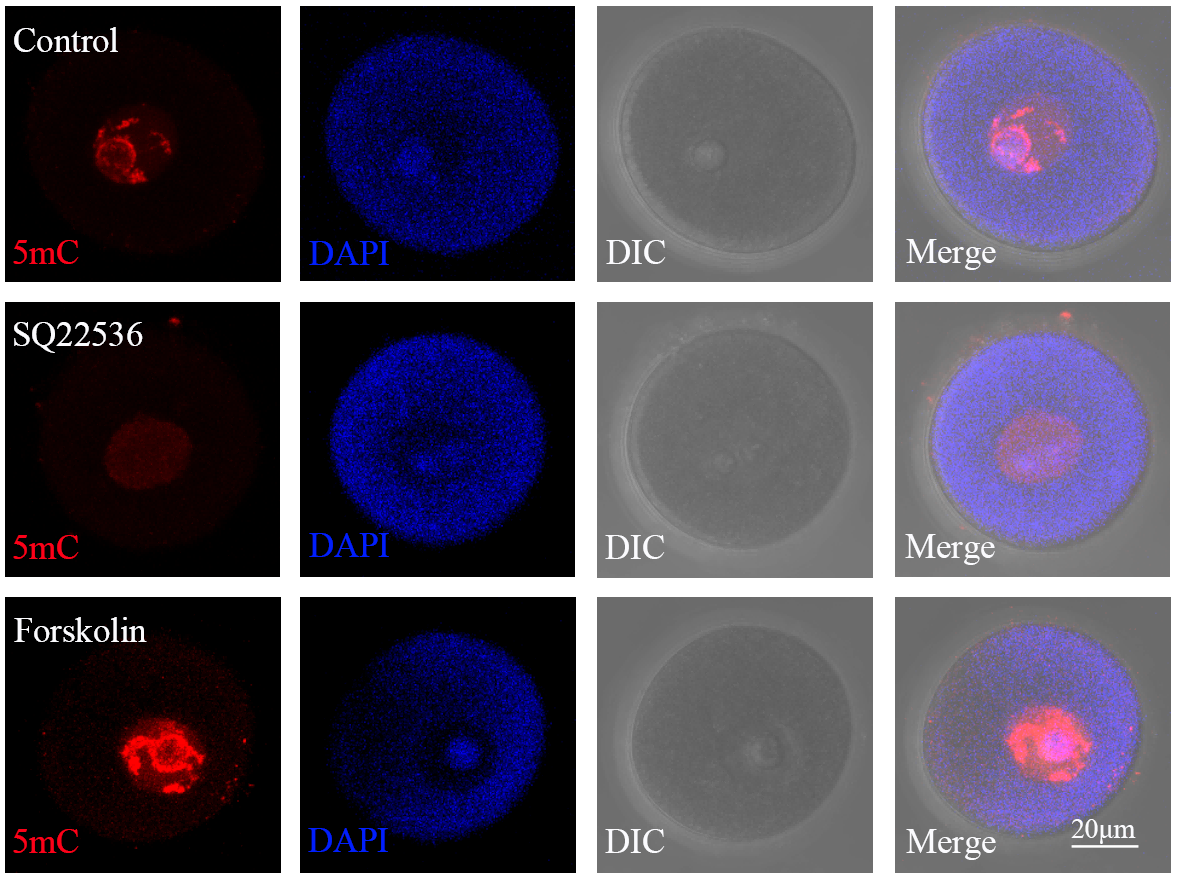
Control
5mC
DAPI
DIC
Merge
SQ22536
5mC
DAPI
DIC
Merge
Forskolin
5mC
DAPI
DIC
Merge
20μm

B

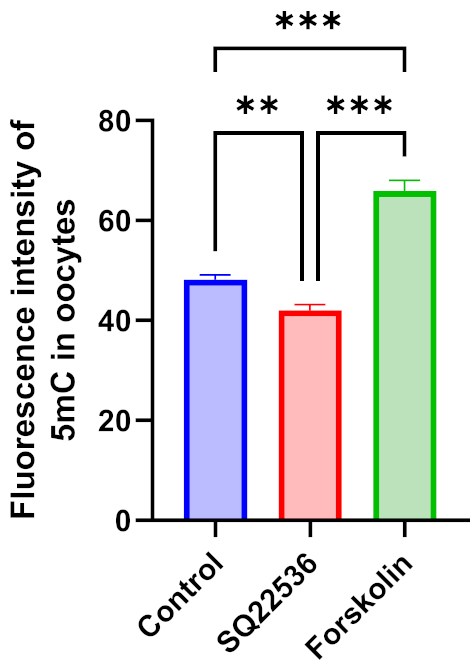
***
**
***
Fluorescence intensity of 5mC in oocytes
80
60
40
20
0
Control
SQ22536
Forskolin

C

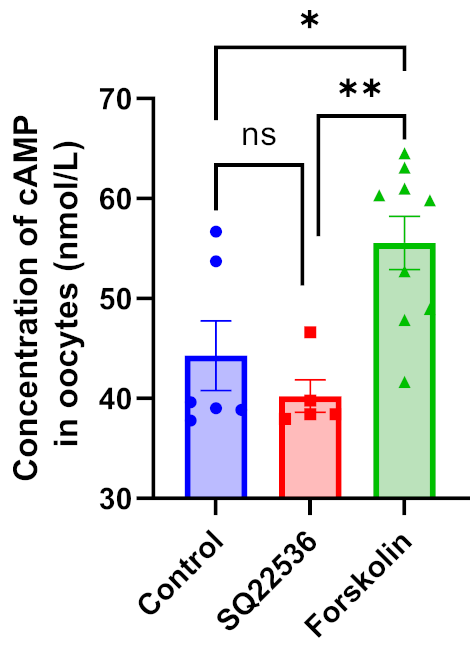
*
ns
**
Concentration of cAMP in oocytes (nmol/L)
70
60
50
40
30
Control
SQ22536
Forskolin

D

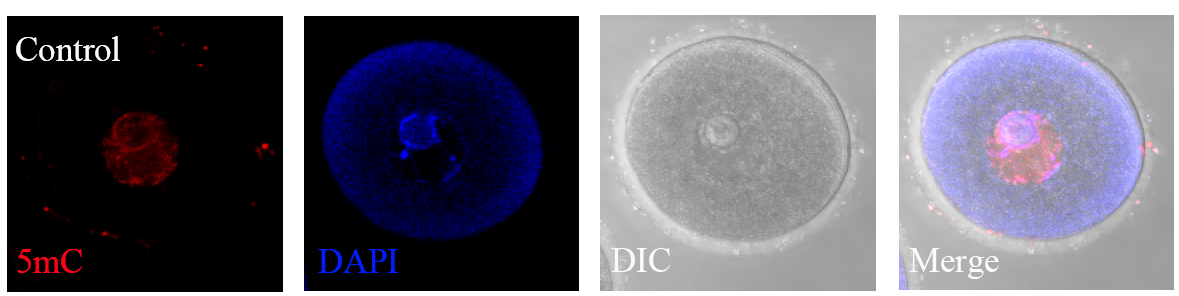
Control
5mC
DAPI
DIC
Merge

F

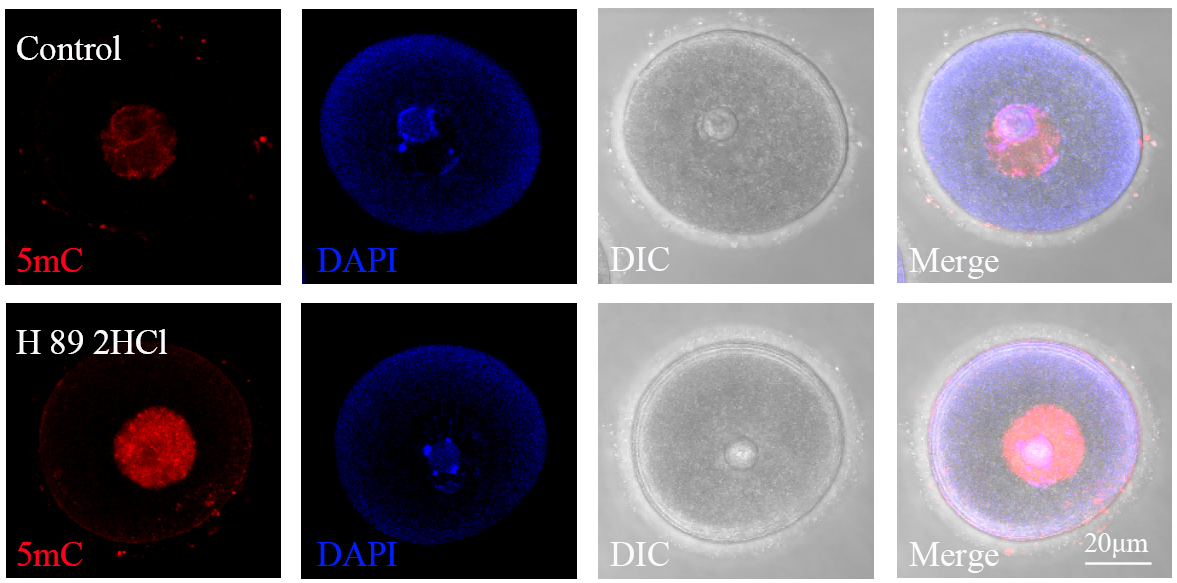
Control
5mC
DAPI
DIC
Merge
H 89 2HCl
5mC
DAPI
DIC
Merge
20μm

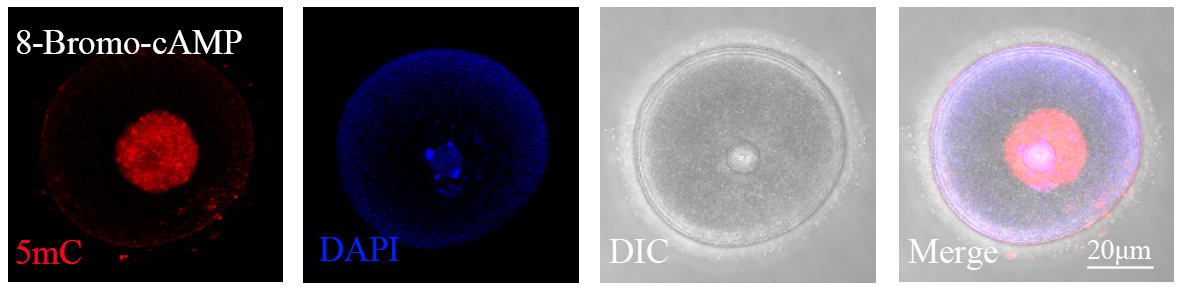
8-Bromo-cAMP
5mC
DAPI
DIC
Merge
20μm

E

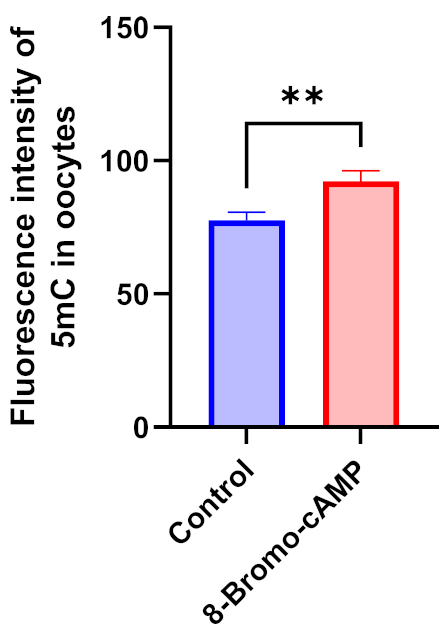
**
Fluorescence intensity of 5mC in oocytes
150
100
50
0
Control
8-Bromo-cAMP

G

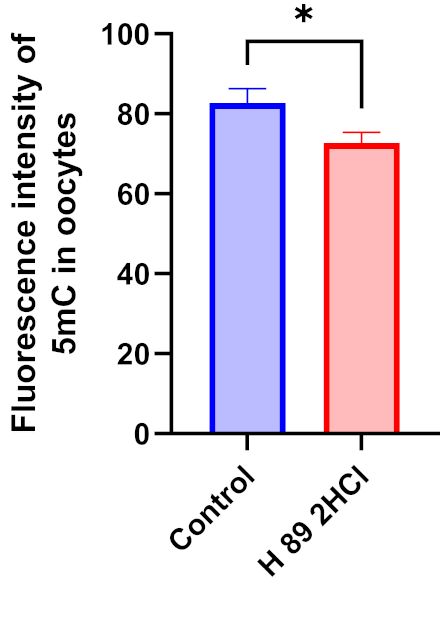
*
Fluorescence intensity of 5mC in oocytes
100
80
60
40
20
0
Control
H 89 2HCl

A

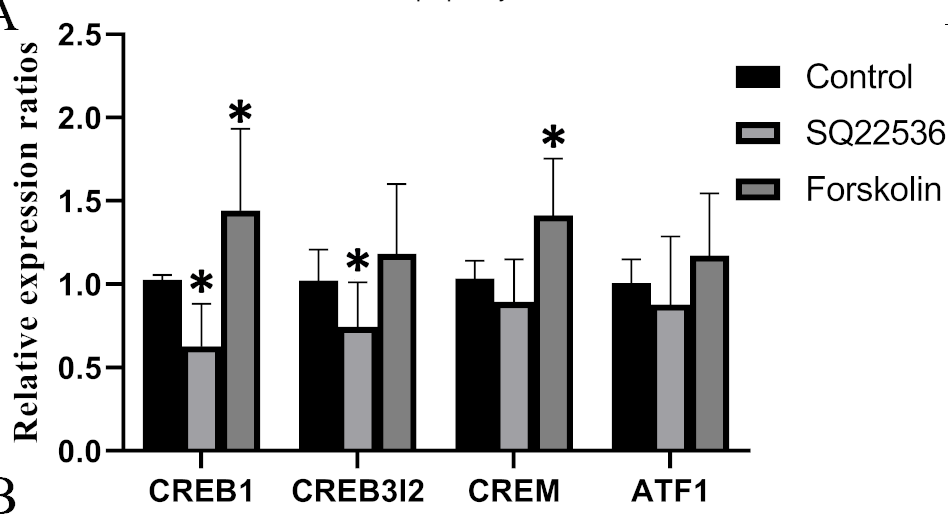


B

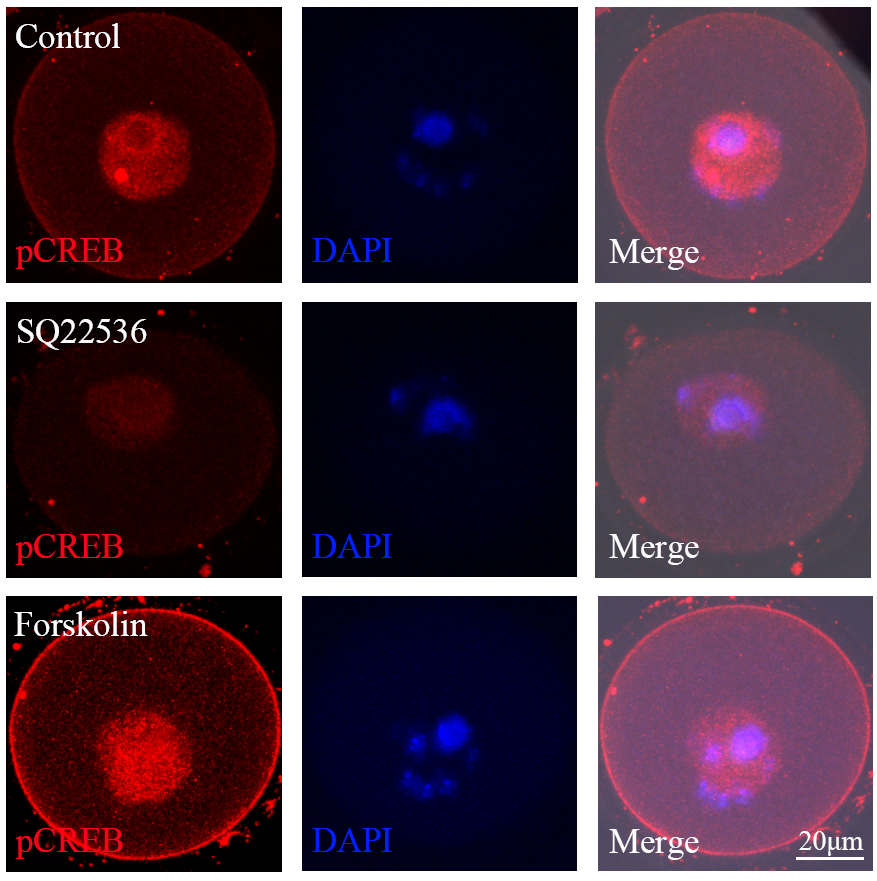


C

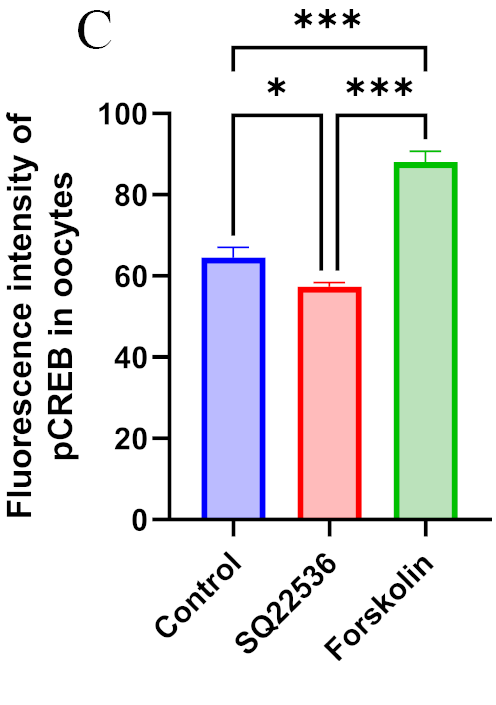


D

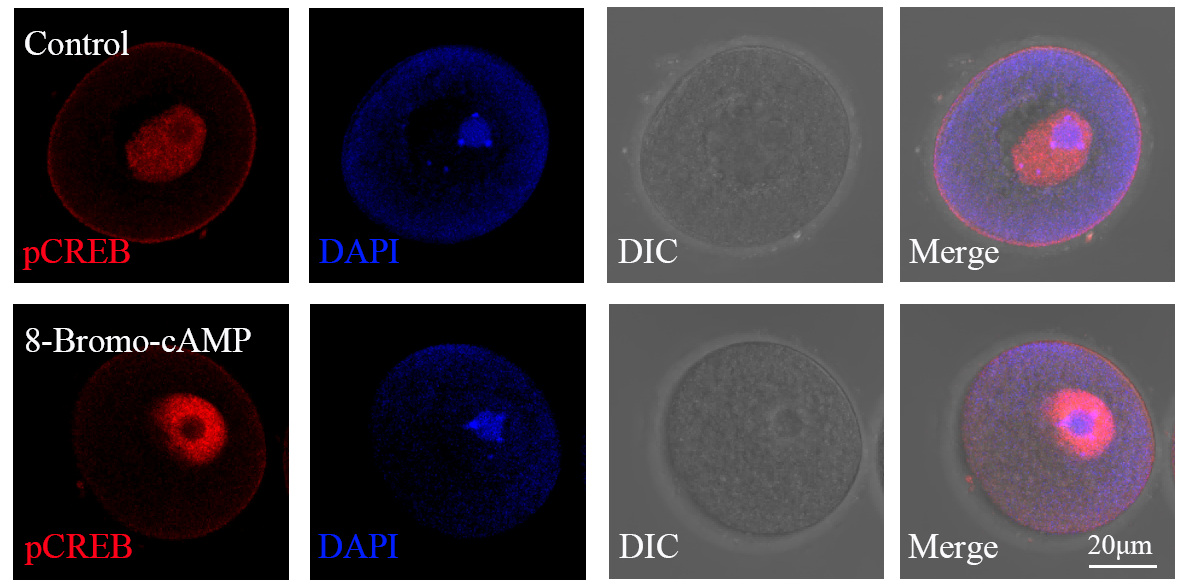


E

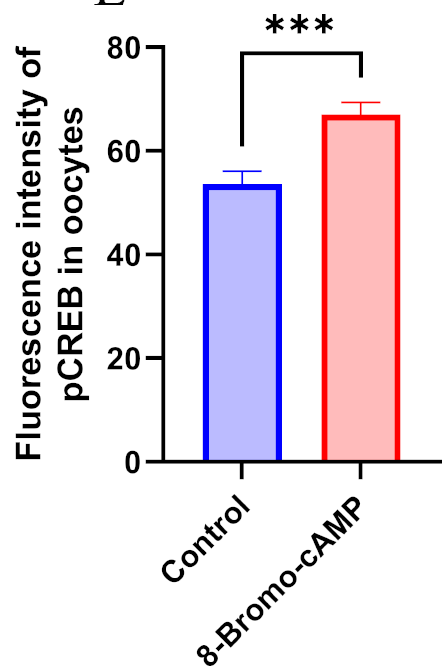


F

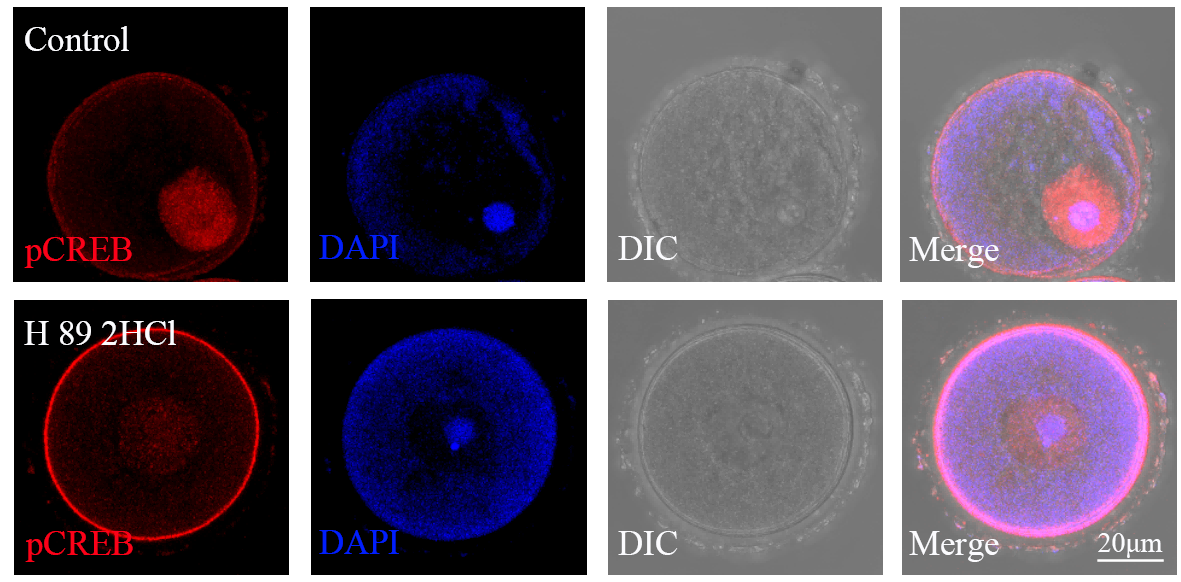


G

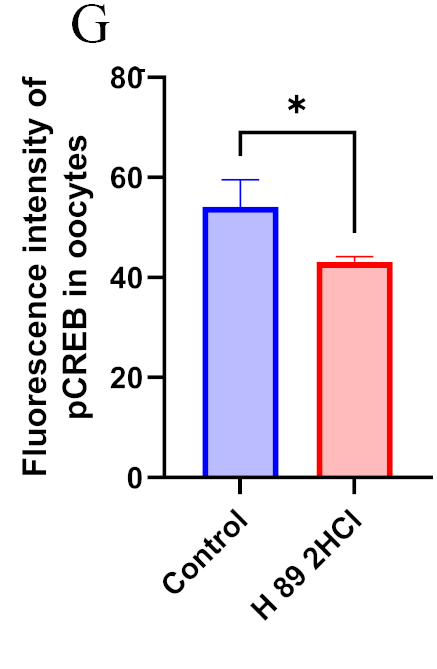

A

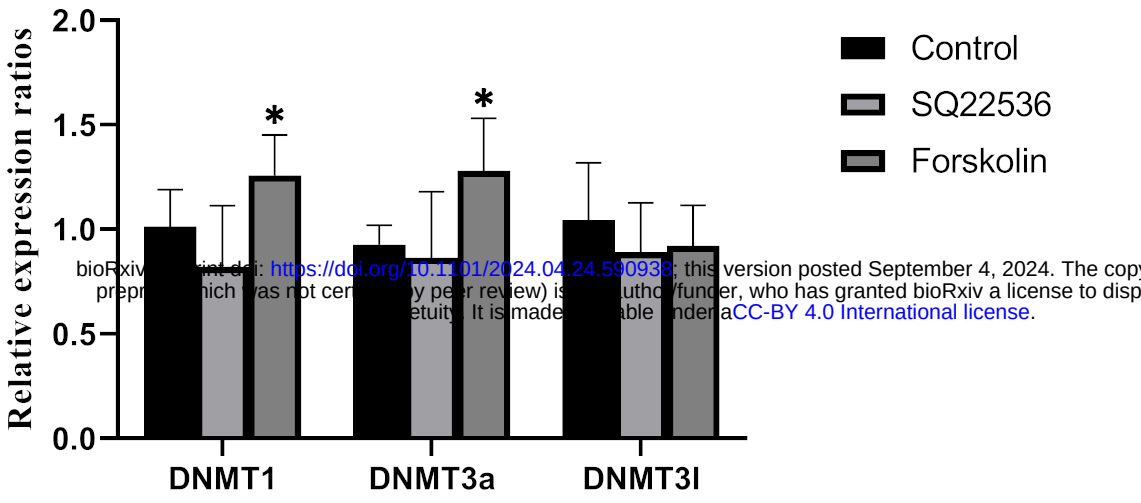


B

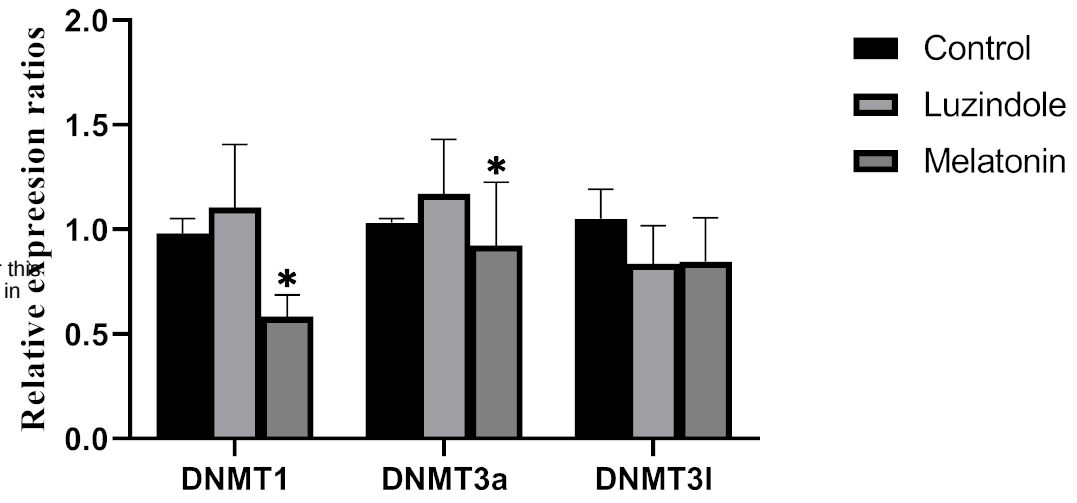


C

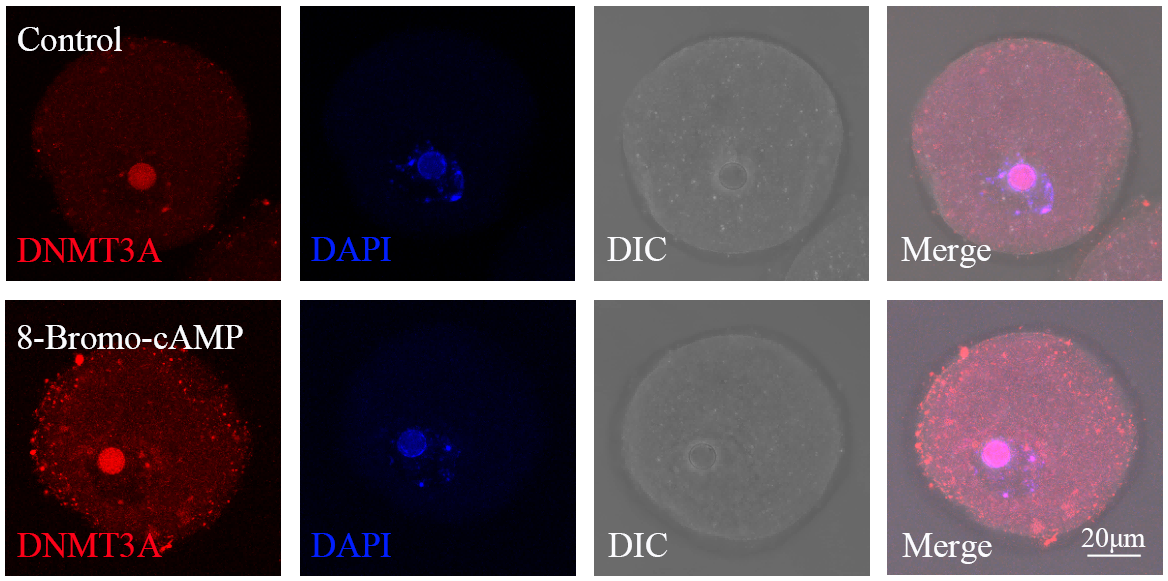


D

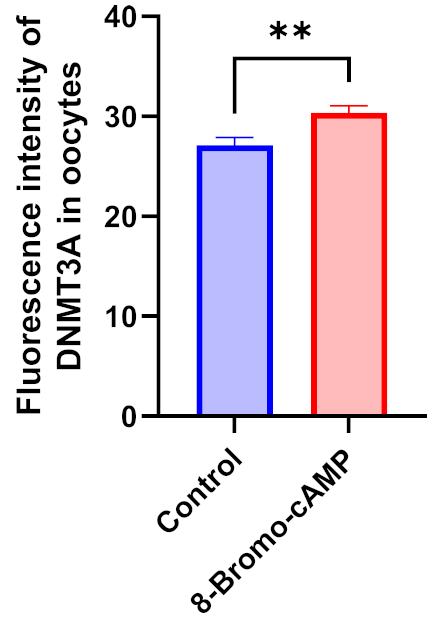


F

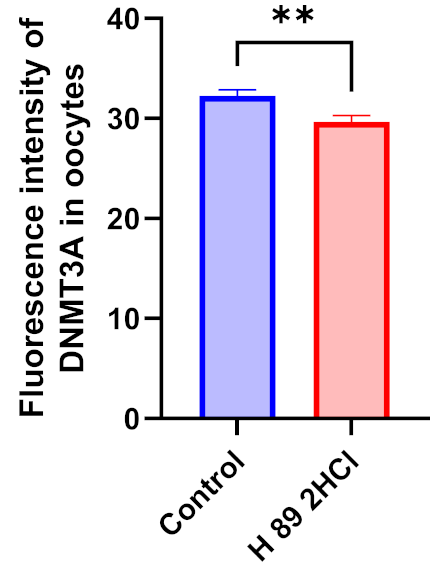


E

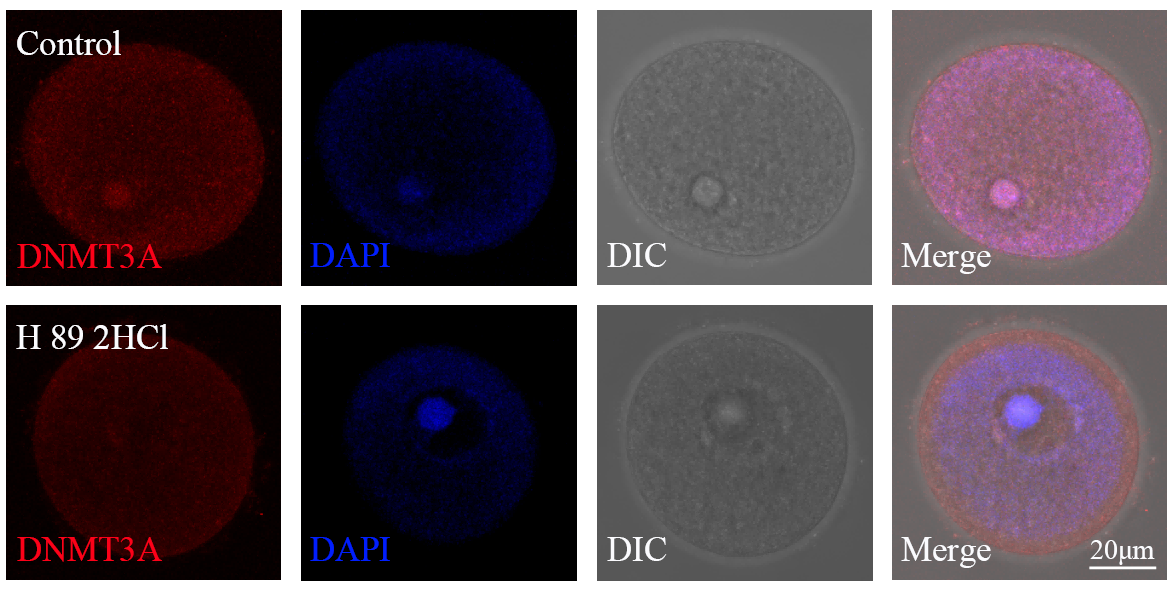


H

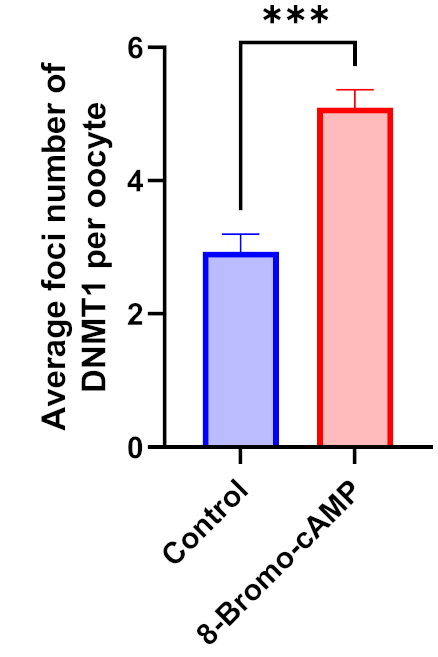


J

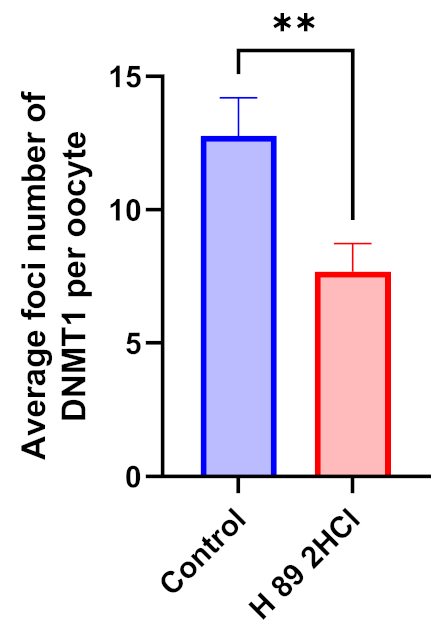


G

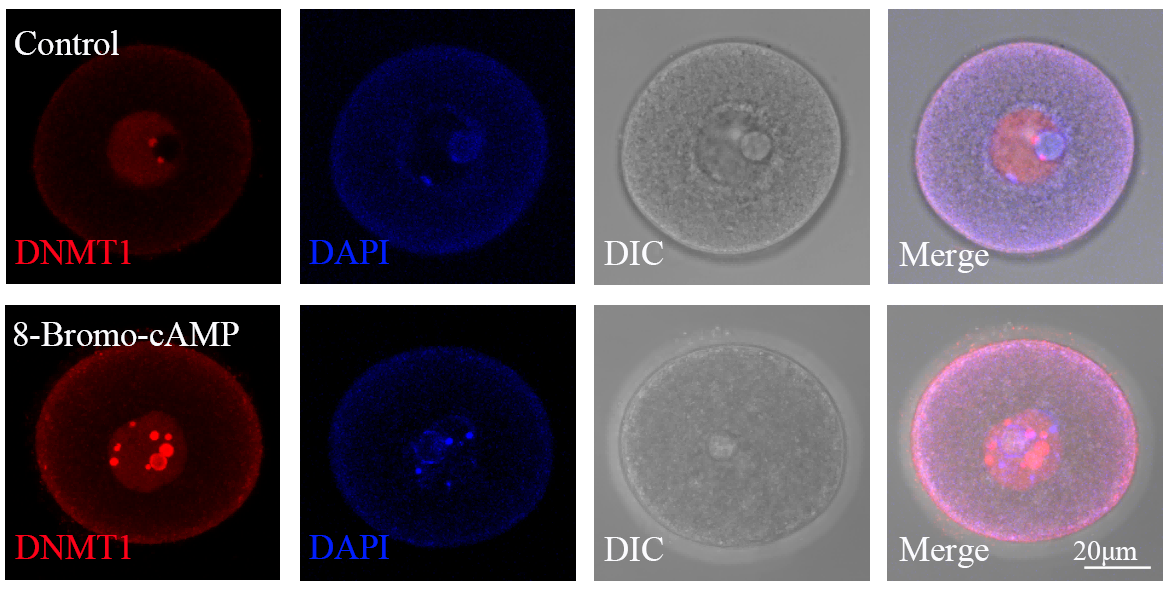


I